East Siberian Arctic Region Expedition '92: The Laptev Sea – Its Significance for Arctic Sea-Ice Formation and Transpolar Sediment Flux

by D. Dethleff, D. Nürnberg, E. Reimnitz,
M. Saarso and Y.P. Savchenko

Expedition to Novaja Zemlja and Franz Josef Land with RV "Dalnie Zelentsy"

by D. Nürnberg and E. Groth

Ber. Polarforsch. 120 (1993)
ISSN 0176 - 5027

Dirk Dethleff, GEOMAR Research Center for Marine Geosciences, Wischhofstr. 1-3, D-2300 Kiel 14, F.R.G.
Elke Groth, GEOMAR Research Center for Marine Geosciences, Wischhofstr. 1-3, D-2300 Kiel 14, F.R.G.
Dirk Nürnberg, Alfred-Wegener-Institute for Polar and Marine Research (AWI), Columbusstraße, D-2850 Bremerhaven, F.R.G.
Erk Reimnitz, United States Geological Survey, 345 Middlefield Road, MS 999, Menlo Park, California 94025, U.S.A.
Mart Saarso, Tallinn Technical University, Järvevana tee 5, 200001 Tallinn, Estonia
Yevgeny P. Savchenko, Arctic and Antarctic Research Institute, Beringstreet 38, 199397 St. Petersburg, Russia.

East Siberian Arctic Region Expedition ´92:
The Laptev Sea - Its Significance for Arctic Sea-Ice Formation and Transpolar Sediment Flux

by D. Dethleff, D. Nürnberg, E. Reimnitz, M. Saarso and Y.P. Savchenko

Expedition to Novaja Zemlja and Franz Josef Land with RV "Dalnie Zelentsy"

by D. Nürnberg and E. Groth

East Siberian Arctic Region Expedition ´92: The Laptev Sea - Its Significance for Arctic Sea-Ice Formation and Transpolar Sediment Flux

by D. Dethleff, D. Nürnberg, E. Reimnitz, M. Saarso and Y.P. Savchenko

1. INTRODUCTION

The Arctic sea ice cover has a large impact on the global climatic evolution (CLARK 1990; UNTERSTEINER 1990). Extension, composition and thickness of the sea ice, its relation to open sea areas and the drift pattern extensively influence gas and temperature exchange between ocean and atmosphere, and thus, the global thermal balance, oceanic circulation and ecology of marine biota (AAGAARD et al. 1985; CLARK 1990). Due to its exposed location, the large seasonal changes in areal extent (12-13 Mill. km^2 in winter versus ca. 6-7 Mill. km^2 in summer), and the small mean thickness (ca. 3 m), the Arctic sea ice cover is thought to react very sensitively even to small environmental changes (GIERLOFF-EMDEN 1982).

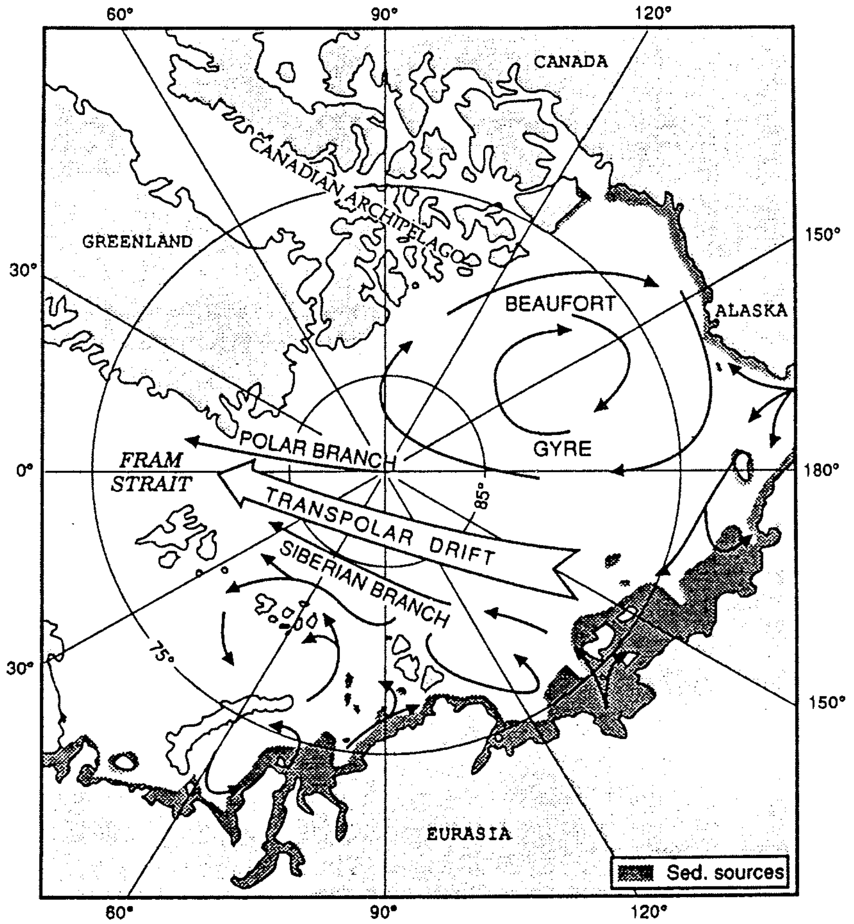

Fig. 1: Ice drift in the Arctic Ocean, generalized after GORDIENKO & LAKTIONOV (1969). Shelf regions shallower than 30 m, where sediment entrainment most likely occurs, are stippled.

The atmosphere and the oceanic circulation transport heat to polar regions, where the energy surplus is compensated by the negative balance between insolation and albedo.

Numerous recent studies have shown that large ice areas of the general Arctic Ocean circulation pattern transport significant loads of marine sediments originating from surrounding shallow shelf regions (Fig. 1). The importance of sedimentary inclusions in the sea ice, when laterally widely dispersed, on albedo (LEDLEY & THOMSON 1986) and subsequently, on ablation processes is still not known sufficiently. Sedimentological investigations suggest that the material transported by drifting sea ice contributes high amounts to deep sea sedimentation during the present interglacial stage. Many observations indicate that the sediment load indeed influences albedo and ablation processes. For paleoceanographic reconstructions, the role of sea ice sediments on the deep sea sedimentation in the Arctic Ocean has to be estimated. To identify a tracer in the deep sea record indicating sea ice cover would thus be of considerable importance.

Under the framework of the BMFT-project "Global Change: The Arctic sea ice - its geological and climatological significance at present and during the past", attempts were made to systematically sample, map and characterize Arctic sea ice incorporations. This includes the quantitative analysis of the lithogeneous, biogeneous and anthropo-chemical components contained in sea ice and icebergs. An estimate of how much sea-ice rafted material contributes to the sedimentation in Arctic regions has been made based on the documentation of the regional distribution pattern and on the assessment on the annual variations in sediment content. This work should eventually lead us to spatially and temporally reconstruct the Arctic sea ice cover during the geological past. Source areas of sea ice and consequently, the processes by which sedimentary material and anthropo-chemical tracers are incorporated there and by which they are redistributed during alternating melting/freezing cycles, are of main interest for the identification of transport paths, ice drift patterns and depositional centers of ice-rafted sediments.

Areas of investigation of the East Siberian Arctic Region Expedition (E.S.A.R.E.´92) have been the Lena Delta and broad shelf areas in the Laptev Sea, since this area is supposed to be one of the main sea ice producing areas where huge amounts of sediments may be incorporated and subsequently transported into the Transpolar Drift. The expedition, which was organized by the Arctic and Antarctic Research Institute (AARI) at St. Petersburg (CIS) in close cooperation with GEOMAR, took place from March 28, 1992 to May 1, 1992. The 5 participants are from GEOMAR, AWI, AARI, the United States Geological Survey (U.S.G.S., Menlo Park, California, USA), and Tallinn Technical University (T.T.U., Tallinn, Estonia). Logistics were exclusively provided by AARI.

The E.S.A.R.E.´92 expedition to the Arctic sea ice source areas is the consequent continuation of sea ice and sea water sampling, after central parts of the Transpolar Drift (Arctic Ocean and Barents Sea) and main ablation areas of sea ice sediments (Fram Strait, Greenland Sea) have already been systematically sampled during RV `Polarstern´ cruises ARK IV, V, VI, VII and VIII. The existing large data set of "dirty ice" has now been expanded by approximately 100 snow samples, 40 ice cores, 20 bottom sediment samples and approximately 40 water samples for chemical investigations. All together, approximately 400 sea ice surface samples and 250 ice cores have been collected during the last years either directly from ship or by helicopter support (Fig. 2). The sedimentological, anthropo-geo-chemical and biological investigation of the samples is still going on. A U.S.G.S. companion project is studying ice rafting in the North American Arctic Beaufort Gyre (Fig. 1). Collected sediments and sediment loads are compared with those at GEOMAR.

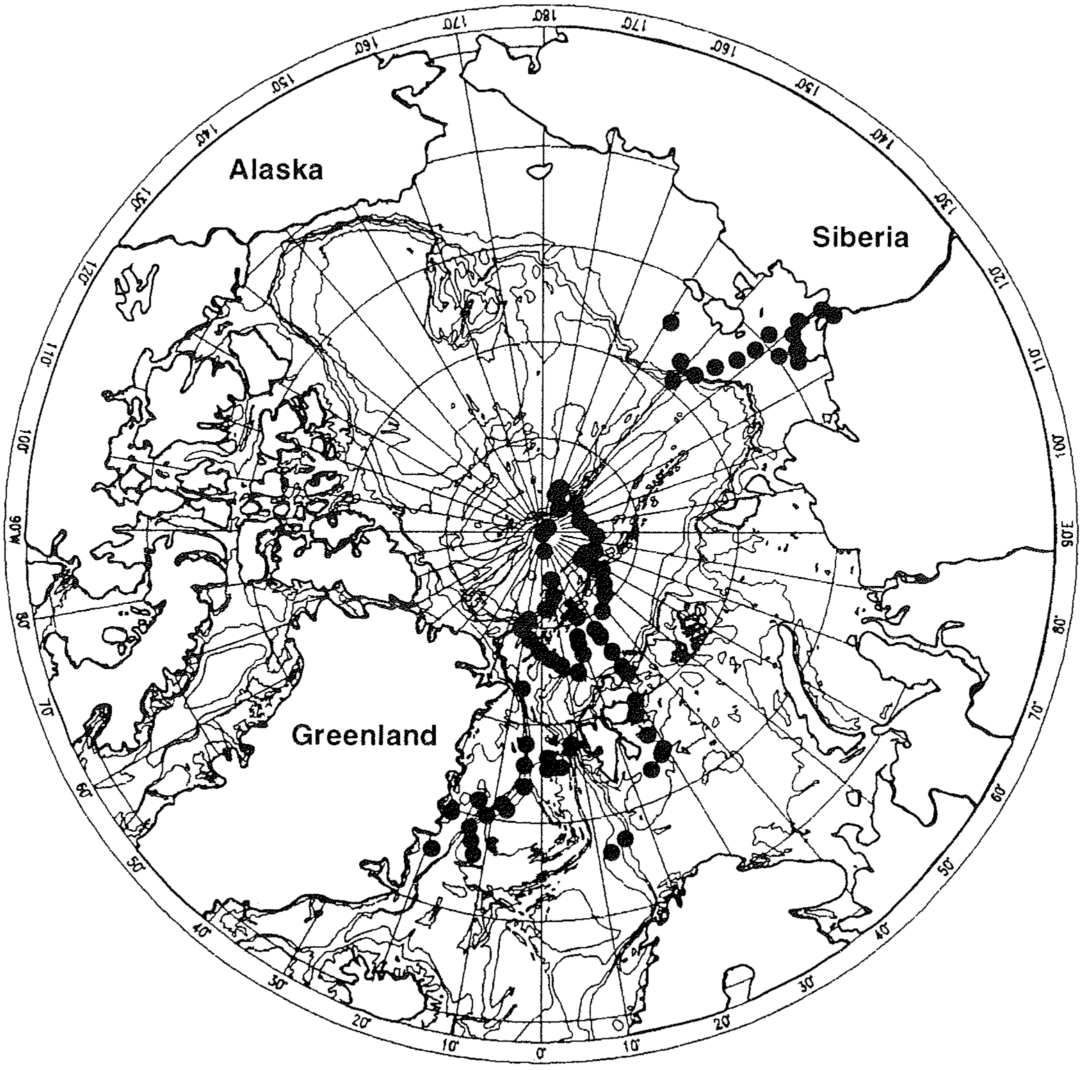

Fig. 2: Bathymetric chart of the Arctic Ocean showing sea ice sample locations.

2. AREA OF INVESTIGATION

Scientific field work during the E.S.A.R.E.´92 winter expedition to Siberia focussed on shelf areas of the Laptev Sea and the River Lena Delta (73-79°N and 122-141°E). Several Lena River and pro delta sites were sampled from the first base camp at Tiksi (12.000 inhabitants), which is located in the eastern Lena River delta. Inner shelf sampling locations, often more than 150 km apart from each other, were reached by helicopter. Fig. 3 shows the geographical positions of 18 sampling sites along an approximately 1000 km SW-NE trending profile.

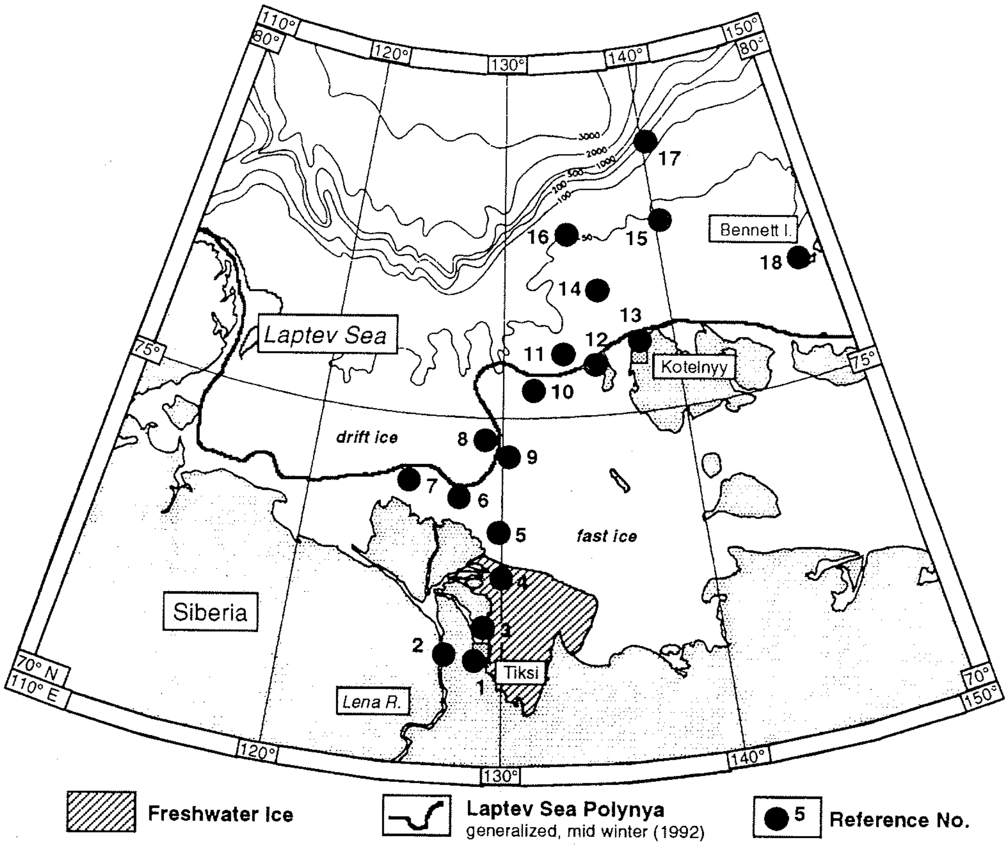

Fig. 3: Location map. The extent of fast ice and fresh-water ice in the study area as observed during April field work is indicated.

The scientific camp was moved from Tiksi to Kotelnyy Island (New Siberian Islands) (Fig. 3) in the northeastern Laptev Sea after 9 days of field work in the delta area. Accommodation during the ongoing 10 days was provided in the "Radionavigational Station Kotelnyy of the Russian Ministry for Marine Transport". From this base camp, the outer Laptev Sea and Central Arctic Ocean (eastern Amundsen Basin) sampling sites were again reached by helicopter.

Bennett Island, an additional field location that attracted international interest in the past decade because of large atmospheric plumes seen on satellite images, was also a target of intensive sampling. Speculations and investigations about the unique phenomenon considered nuclear explosions, breakdown of gas hydrates and release of methane, volcanic eruptions (KIENLE et al. 1983) and meteorological backgrounds (KERR 1992) as possible causes.

3. RESEARCH PROGRAM

Sampling of "dirty ice" for sedimentological, biological and anthropo-geo-chemical investigations was performed along a profile starting on the Lena River southwest of Tiksi, covering the Lena Delta area, and reaching the Transpolar Drift at ca. 79° N and 140° W (Fig. 3, Table 1, appendix). Approximately 60 ice cores with a total length of ca. 120 m and 60 snow surface samples were obtained on 18 stations, which were reached mainly by helicopter support. At least one 10 cm diameter ice core covering the whole ice column was retrieved at each station (Table 2, appendix).

In addition to the ice cores, snow surface samples on the sea ice were taken. Observations on surface characteristics, including thickness of snow cover, relief and floe size were performed routinely. Preliminary investigations on the sediment concentrations in ice cores and surface samples, on the grain size distribution and on qualitative sediment composition have been carried out during field work. Sediment concentrations were determined by vacuum filtering the samples and calculating the weight of sediment per liter of melt water. In order to derive an estimate of the ice floe sediment load, 6-7 ice chunks being representative for the entire ice column were cut from the core and averaged subsequently. The sediment load in snow was averaged from three 1-l samples taken at regular intervals along a line up-wind of contaminating activities on the ice. The sand content was derived by wet sieving of sea ice sediment samples. Further investigations on the sea-ice and snow will include diatom and delta ^{18}O-analyses being carried out at the Alfred-Wegener-Institute for Polar and Marine Research (Bremerhaven, F.R.G.) and the Lamont Doherty Geological Observatory (Palisades, New York, USA).

The sampling of anthropo-geo-chemical pollutants in ocean surface water (1 to 2 m depth) was one of the main objectives during the field work. Analysis will be carried out jointly with scientists from the Department of Marine Chemistry, Institute for Marine Research, University of Kiel (IfM). Certain patterns of sea water and Arctic sea ice pollution are supposed to indicate recent sea ice formation and drift processes in the East Siberian shelf regions and the Central Arctic Ocean. The application of a sea water pumping system especially designed for low temperature operations allowed to obtain ca. 200 l water samples at 5 sampling sites by continuous pumping for about 6 hours (Table 2). The system was installed inside an insolated aluminum box with internal heat sources, which protected against temperatures as low as -30 °C. This unit was set up inside of a tent, and powered by a generator placed some 20 m distant. Filtrates and enrichments of water column organo-chemical pollutants (PCBs etc.) concentrated by this sampling method will enable us to investigate anthropogenic pollution and compare the data to chemical analyses performed by colleagues at AARI. Numerous water samples, in addition, were obtained for heavy metal and delta ^{18}O analyses.

To give an estimate of bottom sediment resuspension which is important for suspension freezing, a sediment trap experiment was carried out in the Laptev Sea flaw lead. A HYDRO-BIOS sediment trap was deployed with collecting area of 0.143 m^2 to 10 m depth (water depth about 28 m) from fast ice edge west of Belkovskiy Island (Ref. No. 12, Fig. 3). The duration of the sediment trap exposure was 54 hours. Surface and bottom water temperatures were measured and water samples were taken for performing salinity determination.

Shelf surface sediments were sampled to a water depth of maximum 64 m. Both a gravity corer (total weight: 50 kg; diameter: 10 cm) constructed by GEOMAR and technicians from the Sonderforschungsbereich (SFB) 313, University of Kiel for use through tiny ice-holes and a small grab sampler were employed. Half liter to one liter volumes of seafloor surface sediments and cores of 10-15 cm length were taken at several sampling sites. Due to cold temperatures (water and air) several gravity corer employments failed. Dumping into the ocean water the supercooled unit (-30 °C) was immediately covered by an ice skin. The parallel sampling of seafloor and sea-ice sediments will probably elucidate entrainment processes. Samples will subsequently be investigated sedimentologically, biologically and anthropo-geochemically. In order to get more information of potential sediment source areas, rock samples were obtained at several land locations.

Parts of the sediment samples mentioned above were prepared for laser grain size analysis to be carried out in the laboratories of "State Oceanographic Institute" (Moscow, Russia, CIS). Grain size distribution in sea ice and bottom surface sediments are supposed to help explain possible entrainment processes of sediment into sea ice.

Ice observations were made during daily field work and during helicopter flights. Visual impressions were documented graphically, photographically and by video techniques. Additionally, four satellite images showing Laptev Sea ice conditions were provided by Russian scientists.

4. BACKGROUND INFORMATION

4.1 The Laptev Sea: Sediment source for the Transpolar Drift?

The shelf edge in the Laptev Sea lies between 50 and 60 m water depths (HOLMES & CREAGER 1974), and as far as 500 km from the continent (Fig. 4). Besides the East Siberian shelf, the area of investigation therefore is the most extensive shallow shelf region bordering the Arctic Basin. According to TOMIRDIARO (1975), these wide Siberian shelves are the result of thaw subsidence from the melting of excess ice in the section, a consequence of exposure to low air temperatures during the last glaciation.

Besides several large submarine valleys, which HOLMES & CREAGER (1974) interpret as submerged extensions of the major rivers in the region, details of the bathymetry have not been released by Russia because of security reasons. Fig. 4 shows an irregular pattern of major shoals with about 10 m relief, some of them reaching close to the sea surface or even breaking the surface. On the Arctic shelf of North America, such shoals are related to the yearly formation of large grounded pressure ridges (stamukhi) or are even caused by these (REIMNITZ & KEMPEMA 1984). The widespread occurrence of small (1-3 m), furrow-like relief forms are thought to be caused by submarine melting of ice wedges and other forms of ground ice (KLYUYEV 1965; TOMIRDIARO 1975; KLYUYEV & KOTYUKH 1985), and therefore also are thermokarst formations. REIMNITZ & BARNES (1987 b), however, have argued that more likely these relief forms here, as of northern Alaska, are due to the frequent plowing of dragging ice keels, and that the various actions of sea ice have much more influence on the formation of Arctic shelves than thermal processes. Grainsize analyses of a few samples from the area show that silty clays to clayey silts dominate, but also show the occurrence of manganese crusts on pebbles and of manganese nodules (HOLMES & CREAGER 1974). These results suggest the occurrence of lag deposits on the shelf. HOLMES & CREAGER (1974) concluded that modern ice rafting is unimportant in the Laptev Sea.

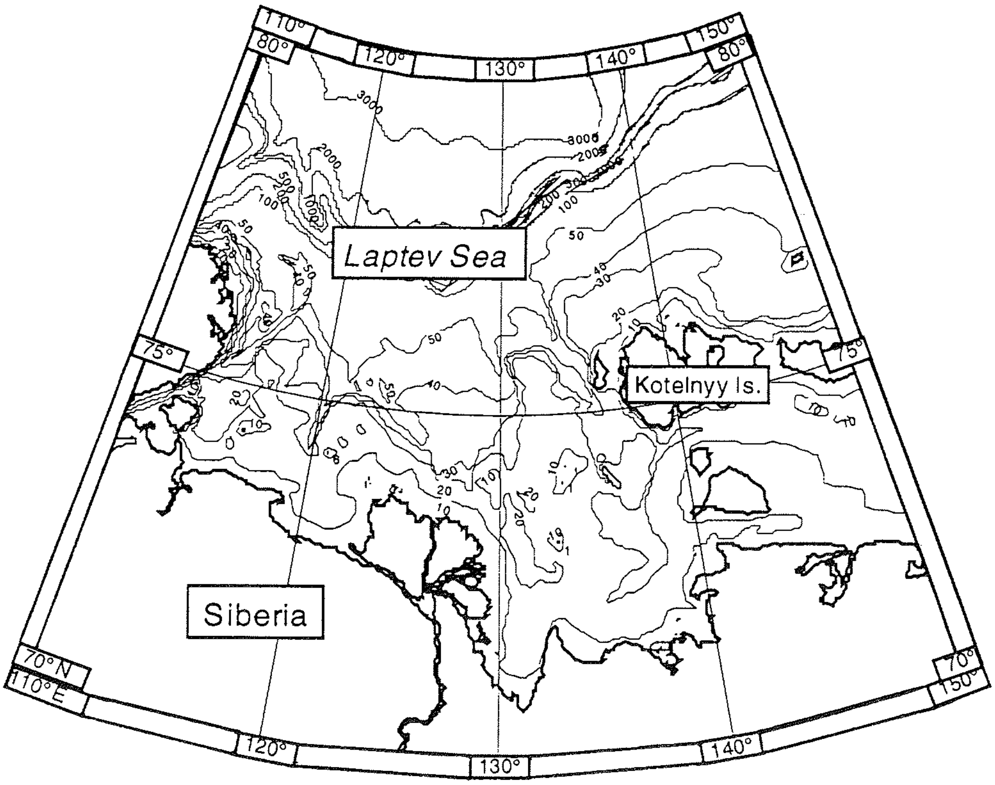

Fig. 4: Bathymetry in meters of the target area, prepared after a map by the Geological Society of America (1986).

A remarkable landform in the Laptev Sea is the large Lena Delta (Fig. 3), suggesting active deposition by the mighty river. Surprisingly, however, the delta shoreline is generally retreating, and the delta therefore is a relict form (for example ZENKOVITCH 1985). The presently low suspended sediment load of about 15 million tons/yr, as compared for example to the 100 million tons of the

McKenzie (MILLIMAN & MEADE 1983), is a partial explanation of the puzzle. But the remaining areal extent of the delta, presumably formed during the Holocene or even during the period since sea level reached its present elevation (about 5,000yrs BP), points to important changes that affected the relationship between continental supply and destructive marine forces during post glacial time.

For 9 months of the year, from early October to July 10 or 20, the Laptev Sea is covered by ice (Fig. 5). It reaches a thickness of about 2 m. The river ice breaks up between June 1 to 10, over a month before the sea ice (Fig. 5). Ships with 10-m draft can navigate in the Lena River. If such great channel depths, when compared to the ice thickness, are connected with the sea, this should allow for sub-ice discharge of spring flood waters. But the literature contains many references of river-water erosion in the coastal zone and deposition of eroded sediments and molluscs on top of the sea ice (e.g. FUCHS & WHITTARD 1930; HOLMES & CREAGER 1974). A satellite image of June 11 (BARNETT 1991) shows that the fast ice along the eastern delta front remains intact while the river channels are ice-free. Evidence for river overflow discharging high amounts of sediment onto the ice, however, is not shown on this image. The so commonly mentioned loading of sediment onto sea ice by Siberian rivers therefore must be questioned, at least for the Lena River. Spring flood waters may actually discharge below the sea ice.

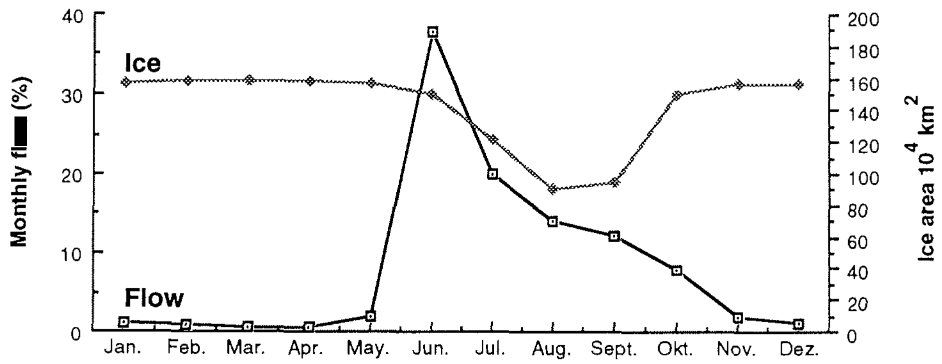

Fig. 5: Comparison of seasonal Lena River discharge variations (from CATTLE 1985) and East Siberian and Laptev Seas ice cover (from MYSAK & MANAK 1989).

Detailed observations about the relationship between river break-up and the sea-ice cover, or even descriptions of the sea ice cover, such as extent of fast ice or location and size of pressure ridge systems, have not been published. Nevertheless, the ice produced in the Laptev Sea is thought to play an important role for the ice budget of the entire Arctic Ocean (COLONY & THORNDIKE 1985). ZAKHAROV (1966) calculated ice-production rates in an important, recurring flaw lead of the Laptev Sea. As defined by him, a flaw lead is an expanse of open water and young ice up to 70 cm thick immediately beyond the edge of the fast ice. But its configuration, location, and size remained unknown. The lack of suitable satellite images to study polynyas in the central Siberian region probably explains why a recent study of Siberian shelf polynyas (MARTIN et al.1989) did not mention that of the Laptev Sea.

KINDLE (1924) thoroughly reviewed early observations of sediment inclusions in Arctic ice and their causes. Recent publications show that sea ice can contain loads of over 1,000 tons/km^2 over extensive shelf regions, far exceeding the yearly supply by rivers to the same area (KEMPEMA et al. 1989). In view of these and other findings, some of the earlier presented entrainment mechanisms, such as bottom adfreezing and slumping from coastal bluffs onto ice, are no longer stressed as important. The Alaskan rivers are not important for long range sediment transport by sea ice, but the suggested loading by the large, and very different Siberian Rivers remains to be investigated specifically. Studies in the North American Arctic show that wind transport of sediment from land to sea is relatively insignificant for ice rafting whithin the Beaufort Gyre (REIMNITZ et al. in press a). PFIRMAN et al. (1989 a) reviewed the possibility of eolian transport from Siberia onto ice as an explanation for the widespread occurrence of fine sediments in the Transpolar Drift. This question is one which we hope can be answered from new data presented here.

Numerous recent publications have shown that fine grained, dispersed, shallow marine sediment inclusions in sea ice are much more important for ice rafting in the Arctic Basin than all other types of inclusions (i.e. REIMNITZ et al. 1987a; KEMPEMA et al. 1989; WOLLENBURG 1991; REIMNITZ et al. in press a). The entrainment process responsible for such inclusions is called *suspension freezing* (REIMNITZ et al. in press a und b), which is driven by the formation of underwater ice. In this process, frazil and anchor ice crystals enclose individual sediment particles and float them to the surface. The requirements for the mechanism are sub-freezing air temperatures coupled with strong winds, open, shallow waters (depth <30 m), and turbulence. Under such conditions, the water temperature drops slightly below its freezing point and triggers the mechanism. It probably is most effective where supercooled waters reach to the seafloor (REIMNITZ et al. in press a). In sea ice the entrainment mechanism of suspension freezing is recognized by the occurrence of rather evenly dispersed fine sediment in an ice layer of 5 to 100 cm thickness, called turbid ice (BARNES et al. 1982; KEMPEMA et al. 1989). Coarse sediment inclusions occur in patches within such ice. This mode of sediment occurrence rules out most other entrainment mechanisms.

Based on these considerations, the principal sediment source regions for ice rafted sediment in the Arctic Ocean are outlined in Fig. 1. Ice volume export from the Laptev Sea is much larger than from the still wider shelf of the East Siberian Sea (ZAKHAROV 1976). These facts, together with sedimentological indications that imply the Laptev Sea as an important source for sediments sampled in sea ice (WOLLENBURG 1991), led to the choice of the present study area.

4.2 The Laptev Sea polynya

The winter ice cover of the Laptev Sea is characterized by the occurrence of an approximately 1800 km long, narrow zone of open water (polynya) on the mid-shelf (Fig. 6). Width of open water varies between 800 m and 4-5 km. Including slush ice, nilas and young ice up to 70 cm thickness, segments of much more than 15 km width are common (Fig. 20).

Flaw leads (and Arctic polynyas in a special sense) during winter are areas of intensive ice formation, salinity increase, convection, and large heat loss into the atmosphere and some distinctive features of meteorological conditions. Springtime is characterized by high accumulation of heat and rapid melting of sea ice (ZAKHAROV 1966). SMITH et al. (1990) distinguish between "latent heat" and "sensible heat" polynyas. Surfaces of "latent heat" polynyas are kept open by continuous loss of latent heat during ice formation. The second mechanism is marked by a flux of sufficient quantities of oceanic heat entering a polynya area, thereby preventing the water surface from freezing. This could occur, for example, in an area of upwelling.

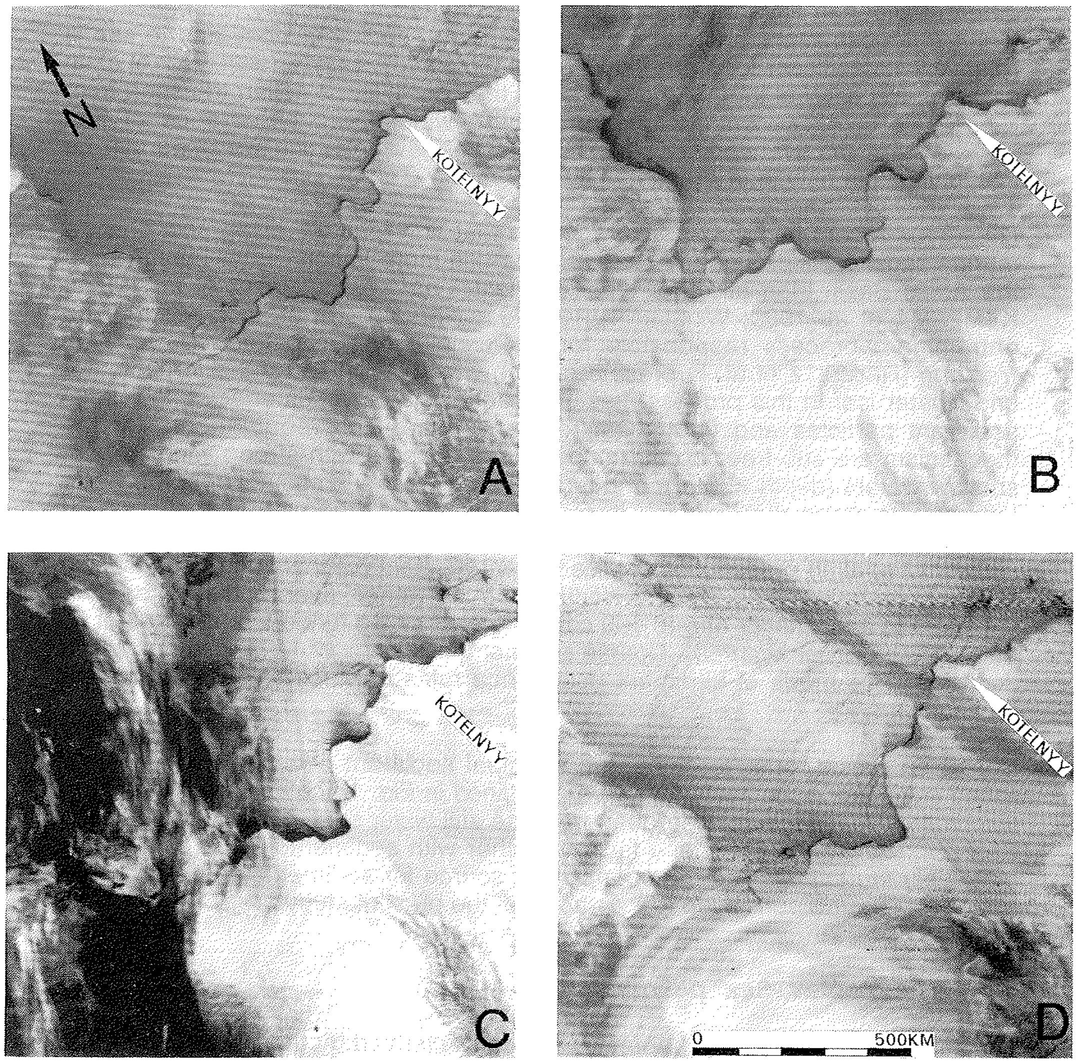

Fig. 6: NOAA-12 satellite images of the study area on A) January 13, B) February 12, C) March 15, and D) April 7, 1992, show the configuration of the fast ice edge, bordered by a very dark belt of open water (polynya) and extremely thin ice (nilas).

Wind drift and oceanic currents that carry away recently formed ice, however, are the main reasons for open water areas on Siberian shelves (ZAKHAROV 1966; SMITH et al. 1990). Meteorological regimes along the entire Laptev Sea coastal area and in the inner shelf region are dominated by mostly offshore winds across the fast ice edge. The long extended Laptev Sea polynya could not be maintained in case of one uniform wind direction for the entire region. Recording of data for each Laptev Sea coastal segment and the inner shelf area would be very helpful for an overview concerning connection between meteorology and ice dynamics. In the framework of E.S.A.R.E.´92, meteorological data recorded every three hours at "Kotelnyy Polar Station, Hydrometeorological Survey of Russia" were copied. Further data for the entire year are requested via AARI from the "Central Meteorological Data Bank" in Moscow.

5. RESULTS

5.1 Meteorological data

Wind velocity and air temperature are important for ice formation and sediment entrainment in the eastern Arctic shelf region. Direction and velocity of strong winds affect ice drift and help maintain the flaw lead (polynya).

Recorded meteorological data from Kotelnyy (Fig. 7) show three principal wind directions for the period of our field work (NE, SE and NW; Fig. 8). Nearly 51% of the time, the wind blew from the northeastern quadrant (0-90°). This occurred during three different periods: April 1-3, 7-9 and 17-23 (Fig. 7). About 50% of these measurements show wind speeds above 6 m/s. The average speed for the three periods is 6 m/s, maxima of 10-16 m/s occurred several times (13% of measurements). High percentages (67%) of wind directions were observed between 31° and 60° (Fig. 8) being nearly representative for all three single periods.

Southeastern wind directions (91°-180°; Fig. 8) dominate in 24% of the measurements and mainly occurred during the periods from April 9-11 and 13-16. Mean wind speed for both periods is 9.8 m/s. Relatively high wind speeds (10-18 m/s) were observed in nearly 50% of measurements. Speeds over 6 m/s were shown in 79% of the data. Graphs for these strong wind events recorded during relatively short time periods (9-24 hrs) partially show parabolic shape (Fig. 9). High percentages (66%) of wind directions between 120° and 150° representative for both periods were recorded (Fig.8, dark grey area).

A third principal April wind direction lies between 270° and 360°, and therefore is directed onshore in Kotelnyy region (Fig. 8). Only 16% of the readings, taken from April 3-7, fall into this category. The computed mean wind speed for the period was 5.5 m/s, with a short period culminating at 10 m/s and higher. Relatively high percentages (57%; Fig. 8) of wind directions between 300° and 330° were recorded during one 24 hr period from 10.00 hrs on April 5 to 10.00 hrs on April 6, with maximum speeds of 7-10 m/s and a mean wind speed of 8.1 m/s.

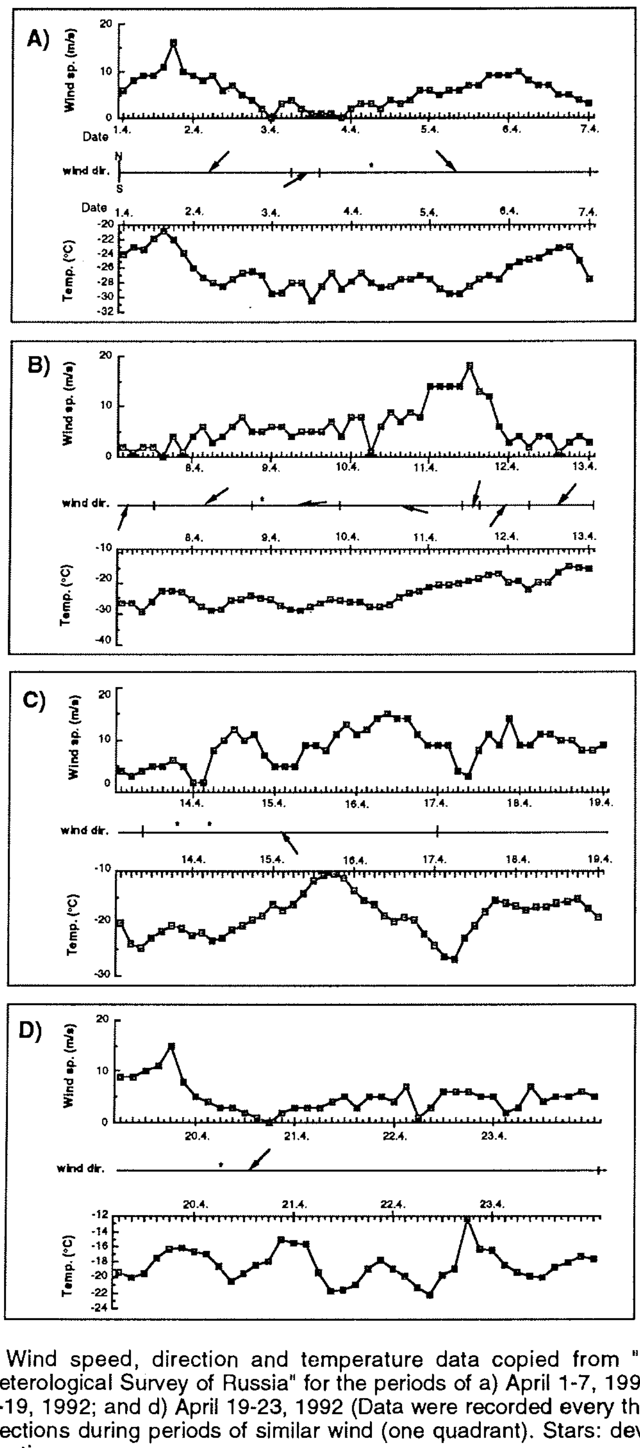

Fig. 7: Wind speed, direction and temperature data copied from "Kotelnyy Polar Station, Hydrometerological Survey of Russia" for the periods of a) April 1-7, 1992; b) April 7-13, 1992; c) April 13-19, 1992; and d) April 19-23, 1992 (Data were recorded every three hours). Arrows: main wind directions during periods of similar wind (one quadrant). Stars: deviations from the general wind direction.

As mentioned above, air temperatures also are important for ice production and sediment entrainment by suspension freezing. Temperatures during the period of recording were always below - 10°C, mostly below - 18°C, and often dropped as low as - 30°C. The lowest temperatures occurred during relatively calm periods (Fig. 7). Temperatures often slightly increased during strong wind periods from different directions.

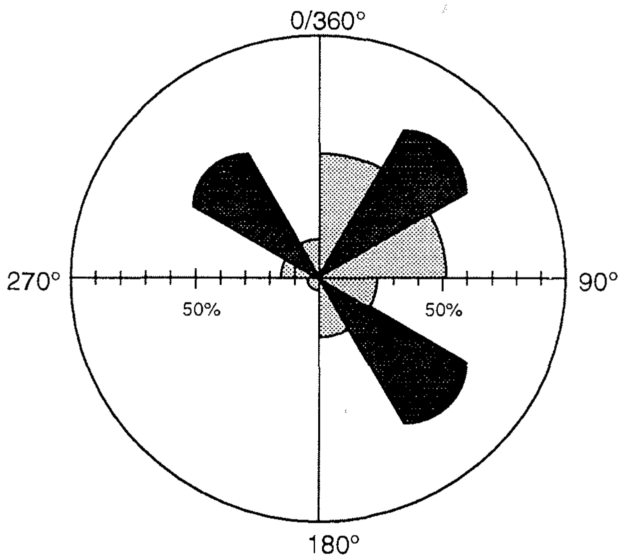

Fig. 8: Main wind directions for the study area and the period of investigation based on data from Fig. 7. Light grey area shows percentages of entire quadrant wind directions, dark grey area shows high percentages of wind directions in a certain range of degree (e. g. 60° to 90°; light grey area taken as 100 %).

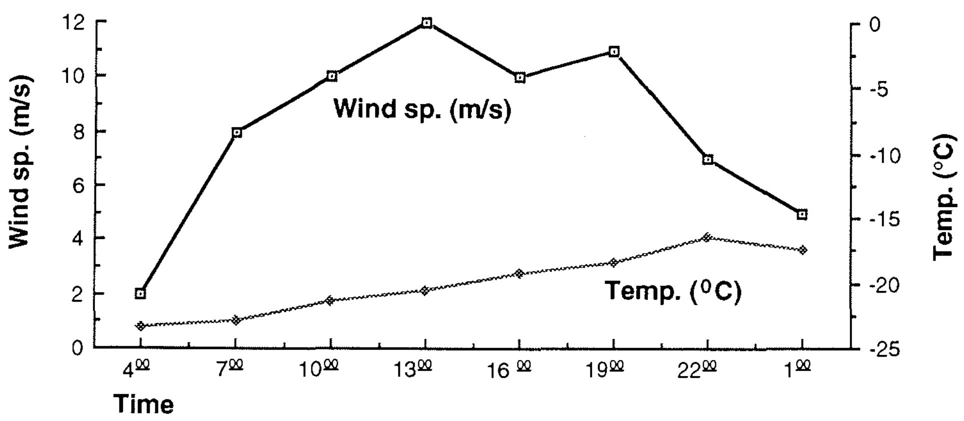

Fig. 9: Graph of strong wind event recorded during a relatively short time period (9-10 hrs, April 14-15) shows a parabolic shape. A significant air temperature increase can be observed.

5.2 Flaw lead and sea ice observations

5.2.1 The flaw lead

The recurring flaw lead, which separates drifting and fast ice and was studied by ZAKHAROV (1966), is shown as a dark band in the NOAA satellite images of Fig. 6, recorded at Tiksi. AARI ice charts for the time covered by these images show nilas to grey ice, or open water to young ice with a maximum thickness of 15 cm, in a rather continuous, 10- to 25-km wide band. During our flights we observed the flaw lead, sometimes only from afar, on different dates and in different areas, extending from the Lena Delta northward beyond the New Siberian Islands. Clouds and a dark fog bank usually revealed the lead from a distance. Wind-parallel streaks of frazil drifting outward from the fast ice edge (Fig. 10) were forming on windy days.

At most crossings of the fast ice edge, and in places were we flew along the edge for some tens of kilometers, we noted a lack of pressure ridges. At some sites a 30 m to 2 km wide belt of 20 to 50 cm thick, smooth ice was attached to 1.5 m thick fast ice. All indications in the areas seen were that onshore pressure has rarely, if ever occurred during the winter, and that outward drift of new ice had dominated. At two crossings of the fast ice edge the lead was closed on the days observed. One was near the northeastern coast of Kotelnyy Island, facing the long-term westward ice drift direction. Here a system of pressure ridges had formed. The other was north of Ref. No. 10 (Fig. 3), along a pronounced bulge in the fast-ice edge. Here a massive pressure-ridge system, with a shearline on the north side, was plotted by GPS navigation exactly on a charted shoal with a crest at 6.6 m below sea level. Ice drift on that particular day was southerly, against the fast-ice edge oriented E/W along this segment of the fast-ice bulge.

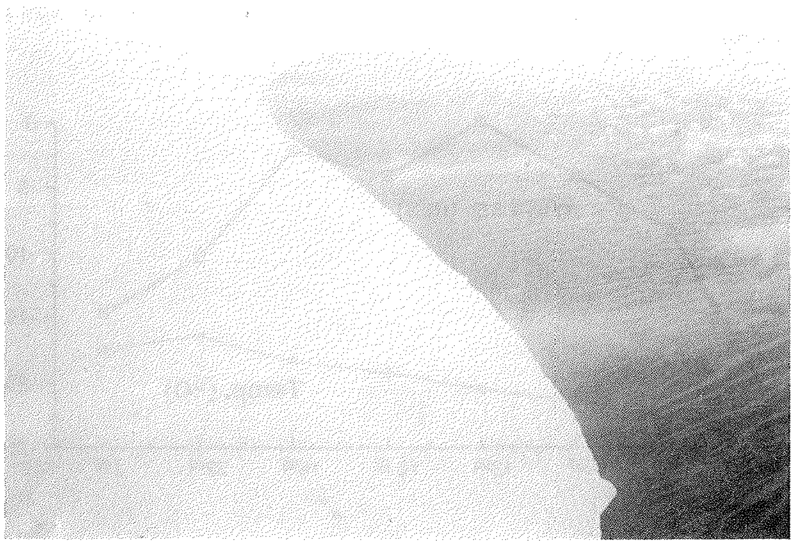

Fig. 10: Light, wind parallel streaks of frazil ice drifting outward from the fast ice edge (left side). Photograph is taken from ca. 150 m altitude. Length of fast ice edge is approximately 3 km.

5.2.2 Extent of fast ice

The development and extent of fast ice are important for sediment entrainment into ice and and its transport. The fast ice becomes firmly interlocked with the coast and attached to the bottom in shallow regions. As it grows thicker and stronger, the fast ice area expands, and rather effectively inhibits further sediment entrainment and movement within its reaches. Only eolian sediment transport onto the fast ice could potentially continue. Beyond the fast ice edge, the ice is moved mainly by wind.

Sequential ice maps prepared by AARI colleagues from interpretations of satellite images (Fig. 11), allow tracking the development of the fast ice cover (Fig. 12). This latter figure shows that in late November, 1991, the fast ice only covered a 10-km wide zone reaching from shore seaward to approximately the 10 m isobath. Only in the area of 145° E, where the 10-m isobath lies far from shore, the fast ice zone had a width of 90 km. In mid December (not shown), much of this wide belt of former fast ice had been removed, but elsewhere its extent was rather similar to that of November.

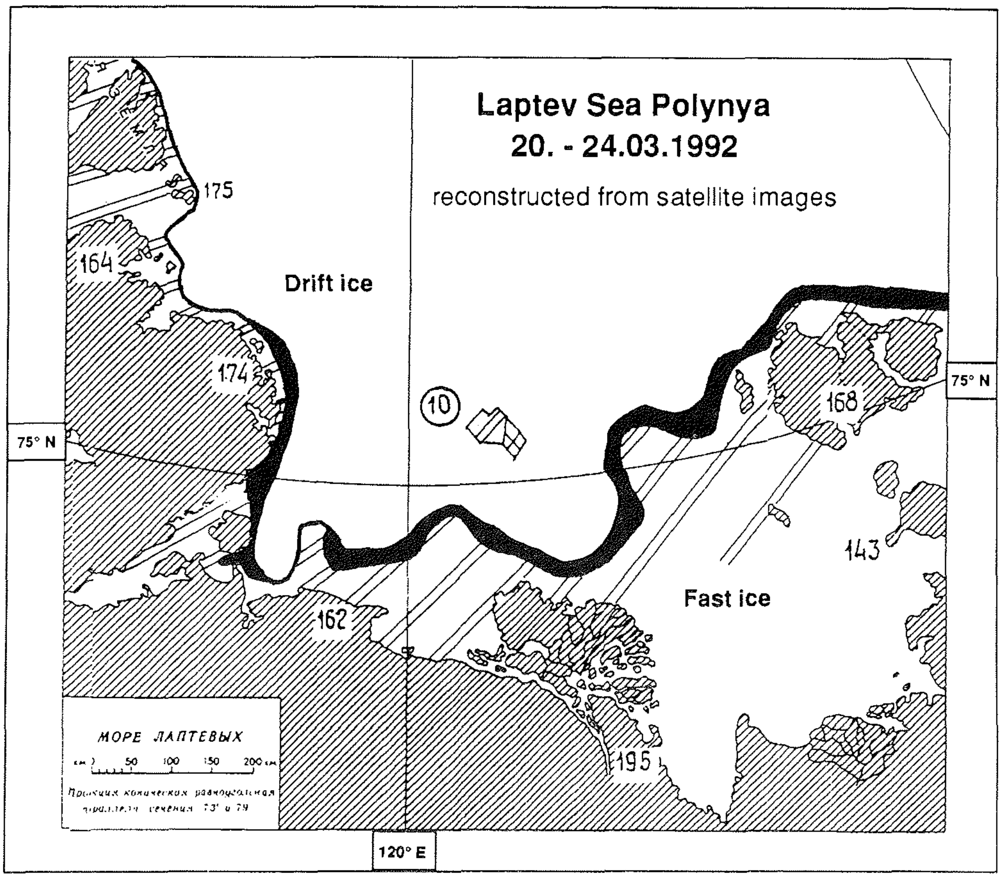

Fig. 11: Ice map prepared from interpretation of NOAA satellite images by AARI scientists (March 20-24, 1992).

In January, February, and March, the fast ice extended out to near the 20 m-isobath, and included as continuous sheet the New Siberian Islands. Locally the configuration of the fast ice edge during these three months seemed to be influenced by shoals. The northern edge of the pronounced bulge in the fast ice boundary during February and March, half-way between the Lena Delta and Kotelnyy, was in the vicinity of the small shoal mentioned earlier.

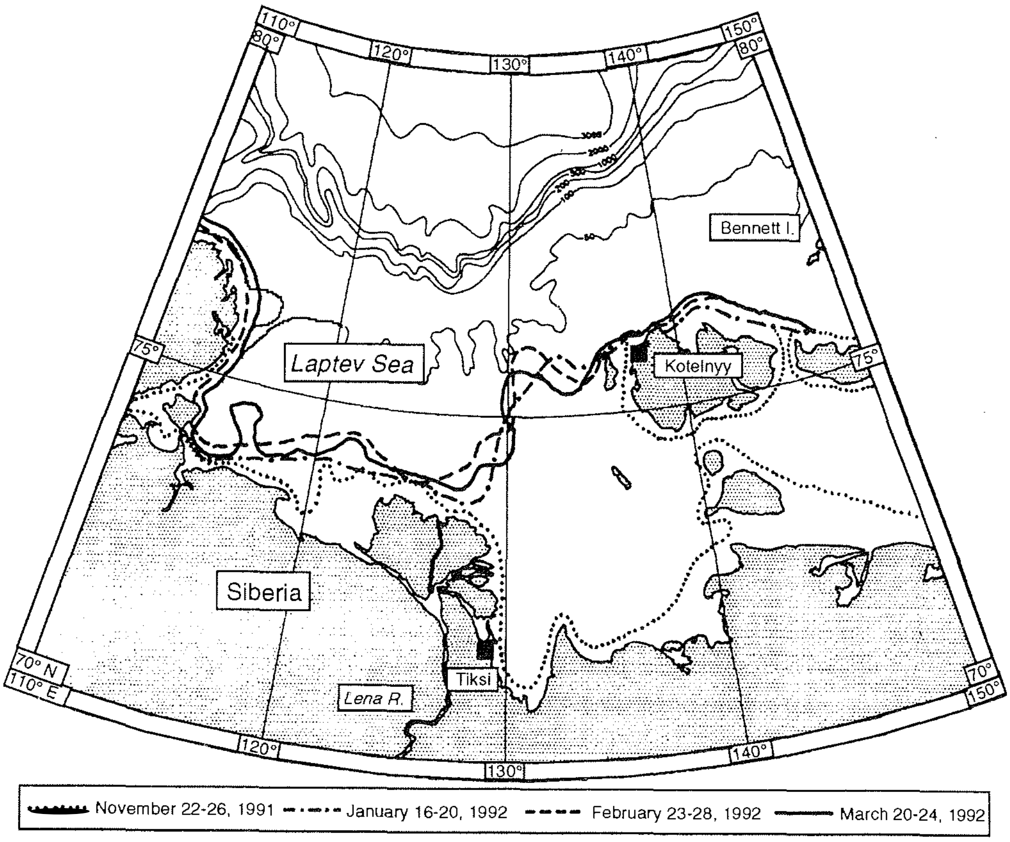

Fig. 12: The edge of fast ice prepared from interpretations of satellite images by AARI scientists. During the period from January through March the outer boundary fluctuated, indicating occasional break-aways due to offshore winds and subsequent accretion of new ice.

5.2.3 Freshwater ice, fast ice and drift ice

The fast ice region included no multi-year ice, demonstrating that the sea was completely ice free during the previous fall. Over large regions the fast ice was rather featureless, lacking pressure ridges and hummock fields. Ten to 40 cm snow cover on this ice precluded observations of any sediment during flights, except for an occasional small ridge exposing broken ice. Most of such ridges looked clean. The smooth fast ice also was found to be clean at most sampling sites. There was, however, a region of turbid ice rubble 10 miles west of

Kotelnyy. A similar turbid rubble field was sampled at Ref. No. 10 (Fig. 3), and others occurred over a 70 km-distance to the south thereof. At the above sampling site the ice slabs typically were 80 cm thick, the upper 30 cm of which was turbid.

For a distance of over 100 km from shore, the eastern pro-delta was covered by characteristic, slick, freshwater ice largely bare of snow, as plotted in Fig. 3. In accordance with the known eastward water flow from the river, such ice was not observed on the northern pro-delta. At Ref. No. 3 (Fig. 3) we sampled the ice in a small, 4.5 m deep coastal lagoon from which the drinking water for the Tiksi military base is pumped. The very transparent freshwater ice of this lagoon contained large amounts of spotty sedimentary inclusions as much as 10 cm in diameter. At about 40 cm depth, a striking layer of gas bubbles 1 to 10 cm in diameter was observed.

All young, thin, drifting ice of probable origin at over 20 m depths within or seaward of the polynya, appeared clean. The ice from Ref. No. 14 northward (Fig. 3) included some multi-year ice, which probably originated in the East Siberian Sea and not the Laptev Sea. At Ref. Nos. 16 and 17 we observed and sampled turbid ice. The lack of surface sediment concentrations on individual slabs of turbid ice sampled indicates it had not yet experienced a melt season, and therefore was first-year ice. Patches of such dirty ice were seen from the air starting at 77°30' N, and in increasing amounts northward thereof.

On a direct flight line from Kotelnyy to Bennett Island we found the lead closed several kilometers NE of the main island Kotelnyy (Fig. 3). At this point we observed a 500 m wide, NW-SE-trending system of pressure and shear-ridges several meters high. Openings in the rather smooth ice several kilometers beyond these ridges revealed that the ice here was mobile, and the system of pressure ridges therefore marked the fast-ice edge. The distribution of open water and compressed ice around Bennett Island itself suggested westward ice drift at the time. From the landing site on a beach near the NE tip of the island we walked 50 m northward into a rubble field of ice blocks 80-100 cm thick. Fifty percent of the ice contained turbid layers 40 to 70 cm thick. In several cases we noted layers of concentrated sediment over turbid ice,

indicating that the ice had been subjected to a melt season and therefore was more than one year old. Repetition of identical sequences of turbid ice overlain by a sediment-rich layer in the cross section of a rubble pile revealed that a 90 cm thick floe with surficial sediment concentrations was "rafted" by compressional forces after the first melt season (Fig. 13).

Flying northward from Bennett Island for 3 km at less than 100 m altitude we noticed the widespread occurrence of patchy turbid ice in the westward drift. From 400 m altitude we had not recognized such turbid ice on the outbound flight. With the knowledge gained directly on the ice and flying low off Bennett Island, however, we were able to recognize locally turbid ice in very recent, snow-free pressure ridges over the entire distance between Bennett and Kotelnyy Islands.

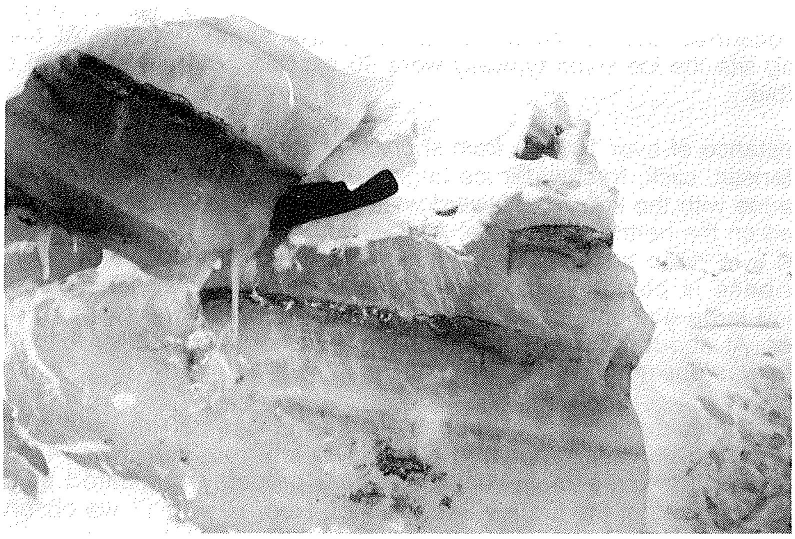

Fig. 13: A 90 cm thick ice flow with surficial sediment concentrations was "rafted" by compressional forces.

5.2.4 Ice thicknesses

At all ice-coring sites except for that in the Lena River channel (Ref. No. 2), the ice floes have been penetrated totally by ice drilling, providing exact ice thickness data. We purposely avoided areas disturbed by pressure ridges, and cored exclusively on flat surfaces. Ice thicknesses in the area of investigation ranged between roughly 0.80 m and 2.37 m (Fig. 14). Except for a few data points, it is possible to establish a geographical trend in ice thicknesses. The fast ice region

is characterized by thicknesses from ca. 1.5 m to 2.0 m. This agrees with the ice chart by AARI for the month of March, 1992, which shows ice thicknesses of 1.95 m in the Lena Delta area, and of 1.43 to 1.68 m in the region west of Kotelnyy Island.

According to BARNETT (1991), thicknesses of the fast ice commonly reach 2 m, and 2.5 m in exceptionally cold winters. Within a distance of 1-3 km from the landward polynya edge, thicknesses decrease to 0.9 to 0.8 m (Ref. Nos. 6 and 8), thinning to values of ca. 0.1 - 0.2 m within 10 m from the fast-ice edge and open water. From the polynya seawards, ice thicknesses increase progressively. At Ref. No. 11, ice thickness amounts 0.98 m, whereas the northernmost sample location (Ref. No. 17) situated within the Transpolar Drift regime already shows an ice thickness of 2.15 m.

An exception from this general ice-thickness distribution pattern occurs at Ref. No. 10, where we sampled the already mentioned rubble field of turbid ice. The ice of the freshwater-reservoir at Ref. No. 3 was 2.15 m, and that of the Lena River was over 1.3 m thick.

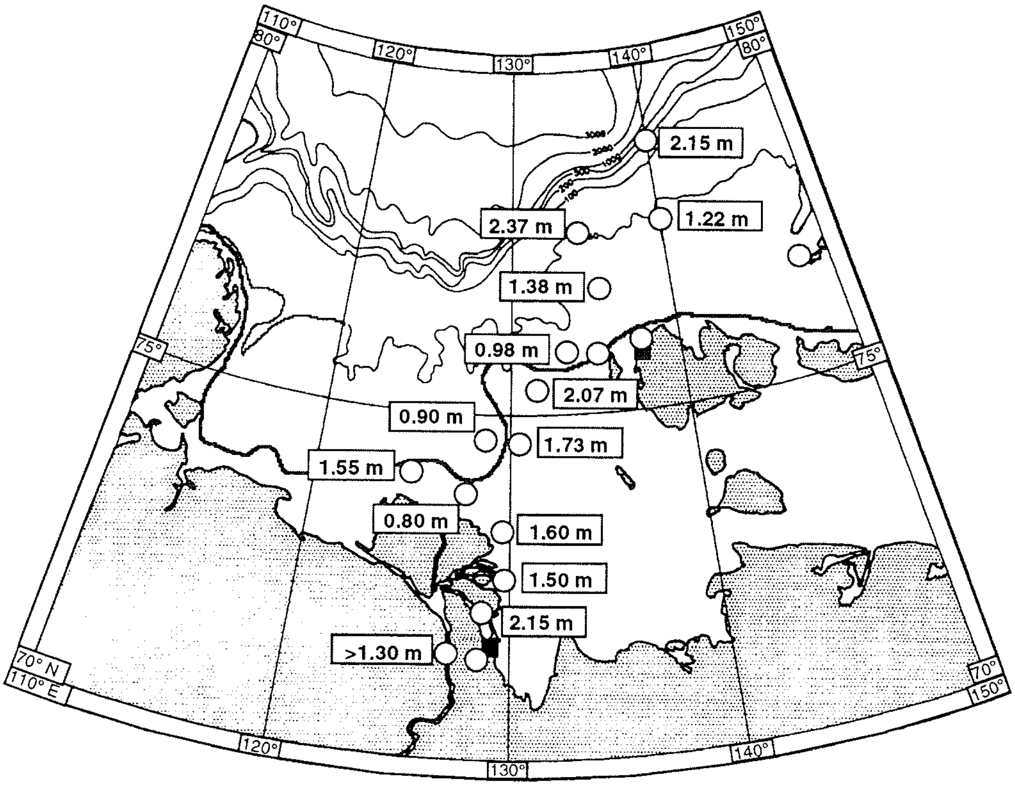

Fig. 14: Bathymetric chart with ice thicknesses indicated by numbers. The location of the polynya is marked by a black line.

5.3 Sea ice sediments

5.3.1 Occurrence of sediments in the Arctic ice cover

Recent sedimentological investigations (THIEDE et al. 1987; WOLLENBURG 1991; NÜRNBERG 1992) show that large areas of the Eurasian Arctic sea ice are covered by particulate matter. Most important mechanisms bringing sediment into the sea ice are summarized in DREWRY (1986), THIEDE et al. (1987) and REIMNITZ & SAARSO (1991). Field observations during the E.S.A.R.E. ´92 expedition reveal that sediment accumulations in the Laptev Sea ice differ from those in the Central Arctic Ocean.

In the Central Arctic Ocean, discolored patches of 10-20 m diameter with diffusely distributed sediment particles in the upper 3 cm of sea ice prevail. Such patches can cover as much as 50 % of the total sea ice surface. In addition, single sediment surface layers directly below the snow cover and multiple layers (10-15 cm thick) within the interior of the ice floes occur. Besides, sediment accumulations within cryoconite holes and sparse sediment accumulations on ridge surfaces have been observed. The latter are mostly restricted to one side of the ridge implying recent eolian transport. The type of sediment accumulations indicate severe redistribution of sediment particles within the multi-year ice due to several freezing and melting cycles.

In contrast, sediment in Laptev Sea ice is distributed diffusely over a broader range of the first-year ice column. This so-called "turbid ice" (KEMPEMA et al. 1989) could be found especially in a region of ice rubble 10 miles west of Kotelnyy , around Ref. No. 10 (Fig. 3), and over a distance of 70 km to the south thereof. Some of the slabs contained delicately structured sediment inclusions (we called them "puff balls"), 5-10 cm in diameter, with sediment and fibrous organic matter, which are strongly suggestive of entrainment by anchor ice (Fig. 15). Evidence for sediment incorporation due to suspension freezing in the polynya, however, could not be observed during April, 1992. Though frazil was generated in the polynya waters and drifted away in bands parallel to the wind direction, the freshly formed slush ice from the air appeared to be free of particulate matter. Layers of sediment enrichment or dark patches of surficial sediment concentrations as in the Central Arctic were not observed, implying that redistributional processes had not been active yet. While the mode of sediment inclusions in the Laptev Sea proper indicated a young age for the ice, that sampled updrift at Bennett Island was older.

The very transparent freshwater ice sampled in the Tiksi drinking-water reservoir contained very many of the delicately structured sediment inclusions already described above. Surrounded by clean ice, these types of sediment inclusion patterns suggest entrainment through anchor ice. High concentrations of similar sediment inclusions were also seen in the ice cover of the Lena River itself (Ref. No. 2, Fig. 3). From the air such ice could be traced for long distances throughout the delta area. Fine to very coarse terrigenous material frozen into the river ice near beaches has been observed, however, is assessed to play only a minor role in the sedimentary budget of the Lena River.

Fig. 15: Image of delicate sedimentary structures entrained by anchor ice. Scale in centimeters.

5.3.2 Potential for eolian sediment transport

Aerial observations were made to determine visually whether the movement of drifting snow also incorporates sediments from exposed land surfaces. The observations were carried out both from the aircraft at 3000 m altitude on the flights between St. Petersburg and the Lena Delta, and from the helicopter at altitudes between 100 to 400 m in the study area. The dominating wind direction sometimes can be detected from the tails of snow originating from larger surface obstacles such as ice hummocks or rock outcrops, and bare surfaces larger than 10 to 30 m also can be recognized from the air. Off northern Alaska, kilometer-long tongues of discolored snow originating from exposed crests of barrier islands have been studied (REIMNITZ & MAURER 1979). Such tails are also connected with sand dunes. Even Landsat images of the Prudhoe Bay oil field show such tails off plowed roads or drilling pads (unpublished observations). Similar findings are not available for Siberian coastal regions. Light conditions to observe such discolorations commonly were excellent during our flights, and exposed ground surfaces were seen even in coastal areas. Signs of eolian sediment displacements, however, were not percepted.

The ice cover of the Lena River itself in the vicinity of Ref. No. 2 (Fig. 3) was an exception. Surrounded by mountains, and affected by 25 knot orographic winds on the day of our study, very noticeable discoloration was observed from an altitude of 100 m along the west bank. Freshwater ice has a very smooth surface compared to sea ice. On this slick surface snow has difficulties to accrete, and therefore large bare spots exist. Sand grains and even pebbles were found in local snow patches on the ice. When placed on slick surfaces, the wind easily propelled such clasts across the ice. The rather steep banks along the shores, on which gravity can move clasts onto the ice, and the slickness of the ice, may explain the occurrence of coarse sediment on the river.

The snow cover in proximity of a windward shore (Ref. Nos. 3, 12, and 13 in Fig. 3) was studied at three additional sites. Only at Ref. No. 13, where patches of bare ground occurred, we noticed excrements of lemings and plant material at a distance of about 30 m from the land surface. Sediment concentrations measured in the snow on sea ice 100 m downwind from land show as much as 34 mg/l (Table 3, appendix). This is not abnormally high, as shown next.

5.3.3 Sediment load

The sediment load (sediment in mg per liter meltwater) in snow samples from the area investigated is generally low and ranges between approximately 0.01 and 200 mg/l (Fig. 16, Table 3). Since these sediment particles occur in fresh snow, they were probably incorporated by eolian transport. A few exceptionally high values between ca. 100 and 200 mg/l were measured in Lena River snow samples (Ref. No. 2), which are mainly due to increased eolian transport (strong orographic winds) and local surface topography. The sediment load of the remaining snow samples never exceeded ca. 50 mg/l. In this respect, snow from fast ice does not differ systematically from that of drift ice samples.

The sediment load in ice cores (Table 4 appendix; Fig. 17) is generally higher than in snow samples. Values range between approximately 0.09 mg/l and ca. 3800 mg/l. The spatial distribution reveals that highest sediment concentrations occur in the northernmost ice cores, which are situated in the Transpolar Drift. Here, values range from ca. 29 mg/l to 800 mg/l. Maximum sediment concentrations of as much as ca. 3800 mg/l were measured north of Bennett Island.

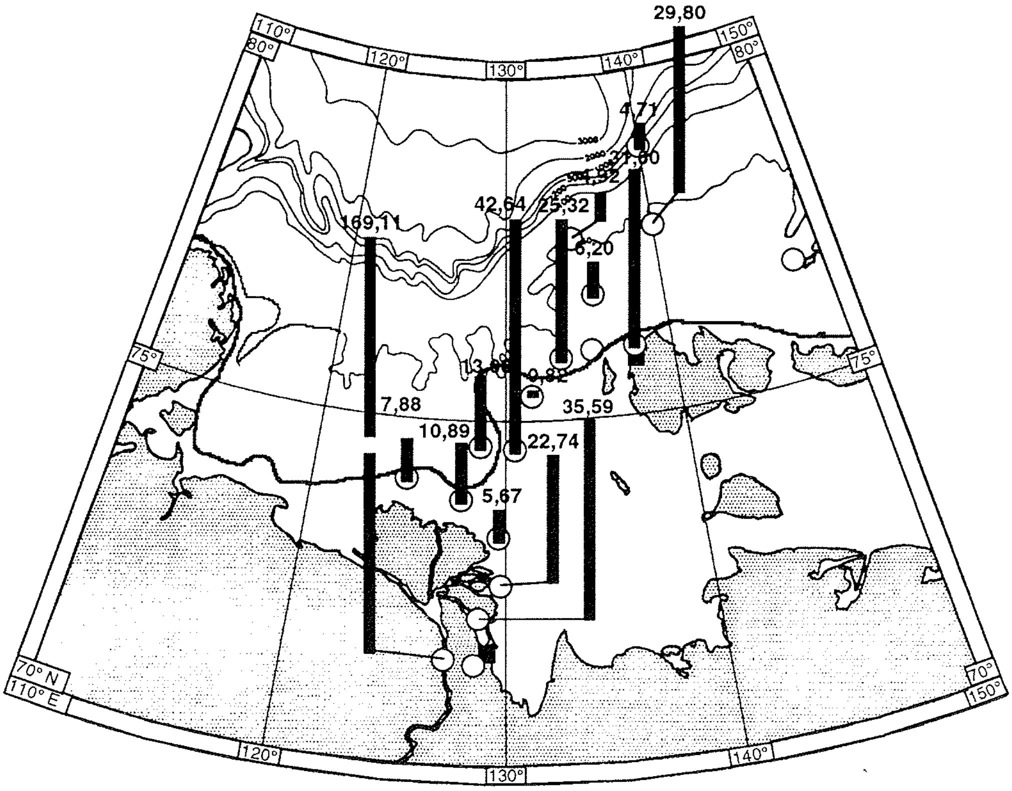

Fig. 16: Sediment load (mg/l) in melted snow, averaged from three samples per site. The edge of the polynya is marked by a black line.

In contrast, ice cores retrieved from the fast ice area have sediment concentrations of only ca. 2.5 to 27 mg/l. Exceptionally high values of ca. 47 mg/l and 262 mg/l were measured in the main Lena outflow, where they are due to high fluvial sediments loads, and at Ref. No. 10 south of the polynya, respectively. Causes for the latter are still unclear to us.

Sediment concentrations found in ice of the Laptev Sea are generally lower than those in sea ice from the Central Arctic Ocean. Here, near-surface concentration values range as high as ca. 57,000 mg/l, indicating that sediments were already concentrated by one or several melting and freezing cycles.

The preliminary grain size analysis carried out by estimation from smear slides shows the dominance of clay and silt fractions (Table 5 appendix, Fig. 18). Sea ice sediments are either silty clays or clayey silts. These observations are consistent with the data set of WOLLENBURG (1991) and NÜRNBERG (1992), who systematically gathered "dirty ice " in the Central Arctic Ocean.

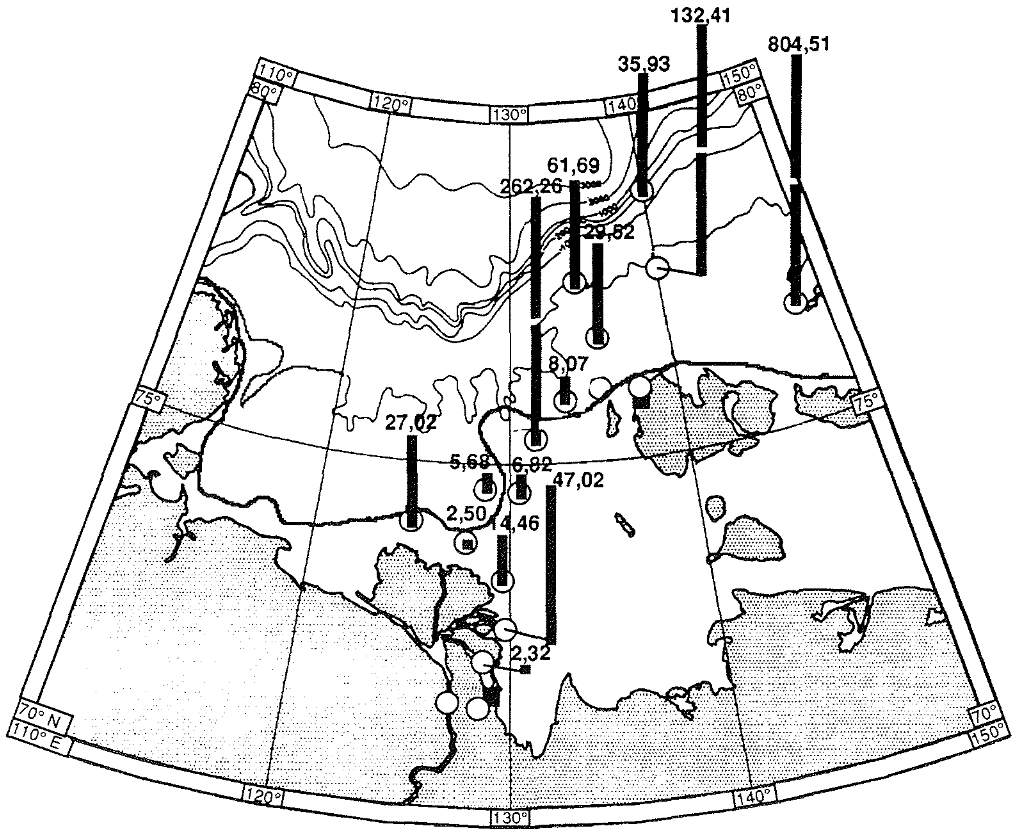

Fig. 17: Sediment concentrations (mg/l) in melted ice cores. The location of the polynya is marked by a black line. Data represent mean values calculated from as many as 7 representative ice pieces per core.

The coarse grain fraction (>63 µm) in sea ice sediments discovered during E.S.A.R.E. ´92 expedition is almost negligible. The concentrations of sand fraction range between 0-36 % of total sample (Table 6 appendix, Fig. 19). In the drift ice and fast ice areas, the sand fraction in turbid ice occurs only in trace amounts or is missing. At Ref. No. 10 however, exceptional high sand portions of up to 36.3 % are present. In contrast to sea ice, the sediments in Lena River ice are dominated by the coarse fraction. Portions of 77.3 - 98.6 % of total sediment have been observed, the causes of which will be discussed below.

The low sand content of sediment in the ice of the Laptev Sea suggests a low energy level during sediment entrainment, perhaps from a suspended state. We believe that entrainment by frazil scavenging from the water column may be responsible for most of the ice-rafted sediment collected. These findings are consistent with the fine grain sizes reported by WOLLENBURG (1991) and NÜRNBERG (1992) for sediments collected from dirty ice in the Central Arctic Ocean.

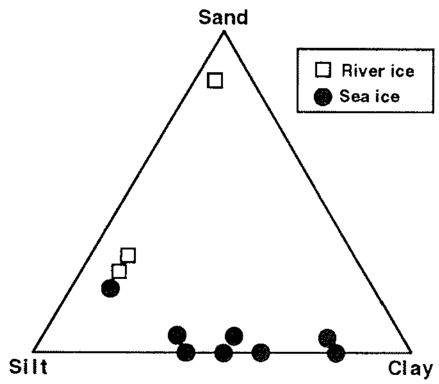

Fig. 18: Grain size investigations of ice sediment samples. Sediments are mainly silty clays or clayey silts. Sand is scarce, and found mainly in river ice.

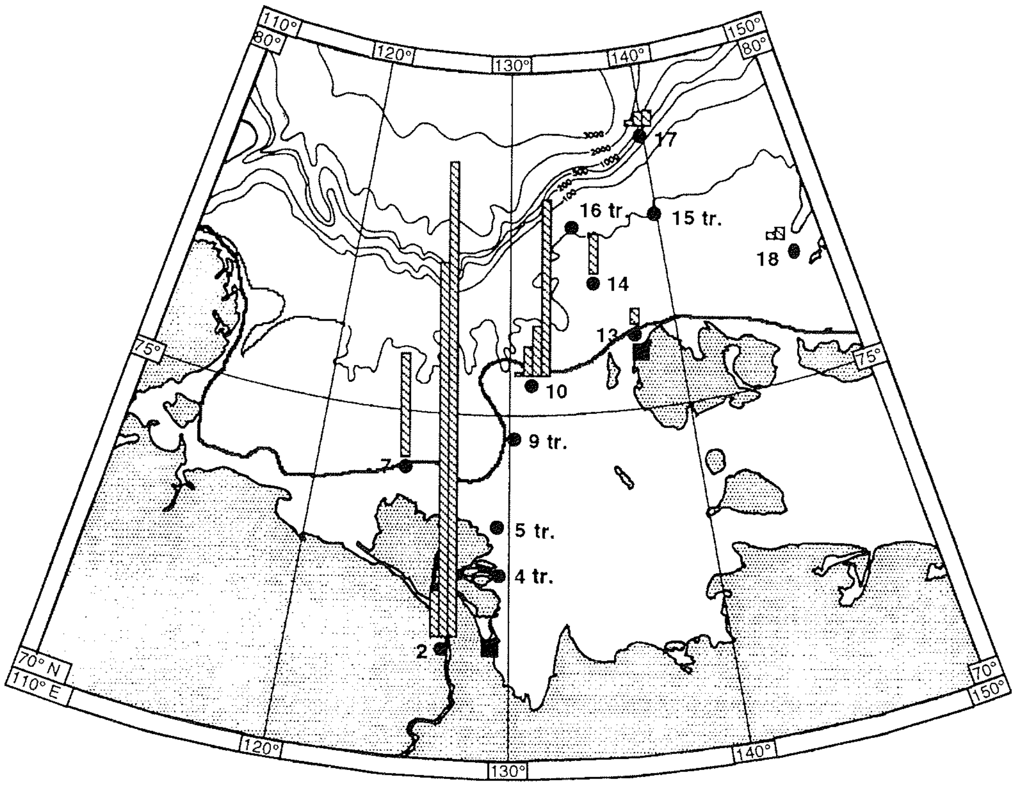

Fig. 19: Coarse fraction (>63 µm) in sea ice sediment samples indicated by hatched bars. Tr. is trace amounts. The longest bar represents ca. 98% sand fraction. Several bars per station simply indicate the variation in sand content.

A systematic component analysis has not been performed yet. However, a brief visual investigation of smear slides (Table 5) reveals quartz, feldspar, rock fragments, mica, clay and heavy minerals to be the dominant terrigeneous sediment components. Biogeneous particles >63 µm are rare being exclusively ostracods and shells. Plant remains could only be observed in ice samples from the Lena River (Fig. 3, Ref. No. 2) and from anchor ice samples at Ref. No. 10. In contrast to ice samples from the Central Arctic, where diatoms have often been observed to be the dominant biogeneous component (NÜRNBERG 1992), the Laptev Sea ice samples are nearly void of diatoms. During the time of sampling, no fluid phases were found in the sea ice due to low air temperatures, prohibiting any diatom growth. Diatom growth was exclusively restricted to the bottom sides of ice floes. At Ref. Nos. 6, 8, 11, 14, and 15 bottom sides of floes were brownish colored indicating the beginning diatom growth in Arctic spring.

5.3.4 Particle flux within the water column

Samples collected in traps during E.S.A.R.E. `92 and the preceding expedition (AMEIS) to the same area in 1991 are still in process. Particle flux values within the water column therefore are not yet available, but preliminary comparisons indicate an order of magnitude higher flux in 1991. Both traps were deployed 10 m below the sea surface at the edge of the fast ice, the first one NW of Kotelnyy, where the water depth is 17.5 m, the second one at Ref. No. 12 (Fig. 3), where the water depth is 28 m. The much higher particle flux at the shallow site in the flaw lead supports the belief of ZAKHAROV (1966) that the convection depth in the polynya of the southern Laptev Sea does not exceed 22 m. As knowledge of entrainment by suspension freezing in the seasonally shifting polynya is crucial for this study, the need for further work on particle flux and convection depths is obvious. *In situ* water column temperature measurements showed surface values of -0.65° C and near bottom values (27 m) of -0.55° C.

5.4 Anthropo-chemical pollutants in the Laptev Sea

Results of anthropo-chemical pollutant studies are not available yet, but those of the 1990 AARI research program are shown in Table 7. Compared to the Baltic Sea, one of the most polluted bodies of world ocean waters, the AARI investigations show relatively high concentrations of PCB, HCH, DDT group (DDT, DDD, DDE) and PHC (petroleum hydrocarbons) in Siberian shelf water masses and the ice cover.

Table 7: Mean annual concentrations of pollutants in Siberian shelf areas (MELNIKOV & VLASOV 1990)

	Concentrations	
Pollutants	Sea Water	Sea Ice
PCBs	1.00 ng/l	2.00 ng/l
HCH	1.66 ng/l	1.18 ng/l
DDT	0.46 ng/l	0.41 ng/l
PHC	15.5 µg/l	16.2 µg/l

River discharge and waste waters of coastal industrial settlements are primary contributors of chemical pollutants into Arctic shelf water and sea ice cover. Extensive yearly sea ice export from the Laptev Sea to the Central Arctic Ocean thus could be responsible for a widespread distribution of chemical pollutants.

Concentration and distribution patterns of anthropo-chemical pollutants are believed to record recent ice formation and drift processes in the entire Eastern Arctic Ocean (Siberian shelf area, Central Arctic Ocean, ablation areas). Re-identification of anthropo-chemical ice inclusions in the entire Arctic Ocean is supposed to give references to Arctic sea ice drift patterns and will be a focal point of further investigations.

6. DISCUSSION

The ice regime of the Laptev Sea is very different from that of the Beaufort Sea, where most past studies of sediment entrainment, load, and transport by sea ice were made (KEMPEMA et al. 1989 and REIMNITZ et al. 1987). There, the clockwise rotating Beaufort Gyre, and winter winds that blow obliquely onshore, result in ice convergence, pressure, and formation of the stamukhi zone characterized by massive grounded pressure ridges at 20 to 40 m water depth. Except for a short, recurring polynya in deep water off the MacKenzie, there normally is no open water on the shelf during winter. Sediment entrainment therefore occurs with the last, open and shallow water of the summer. The Laptev Sea, on the other hand, is an area of ice divergence, emphasized by an 1800-km long, recurring flaw lead along the fast ice edge. This edge is not stabilized by large, grounded pressure ridges. The flaw lead therefore is a highly dynamic feature, in which mid-winter sediment entrainment by suspension freezing might be expected to occur under suitable weather conditions.

6.1 Effect of atmospheric circulation on ice generation and drift

Kotelnyy meteorological data show a close relation to local ice formation and ice dynamics in the Laptev Sea polynya. Due to wind speeds mostly exceeding 6 m/s and temperatures almost constantly below -15 °C, continuous ice formation occurred during the field period in April. Depending on predominating local wind directions, recently formed ice is carried away from or towards the fast ice edge. Northeastern winds drive ice nearly vertically towards the fast ice edge north off Kotelnyy Island. Here, the flaw lead was observed closed during helicopter flights on April 23 after a 6 day period (April 17 to April 22) of strong northeastern wind. The open water area west off Kotelnyy Island at the same time is characterized by transport of young ice nearly parallel to the fast ice edge and against the northern edge of the bulge further to the south. This was observed on an April 22 flight across the windward edge of the fast ice bulge north of Ref. No. 10, where the drift had closed the lead and compressed the ice into ridges.

During a 4 day period of northwestern wind in early April (3 to 7), and before our arrival in the area, the polynya evidently was closed west of Kotelnyy Island. A Landsat image recorded on April 9 (Fig. 20) shows this. It was taken after two days of strong northeastern wind (April 7 to 9), which re-opened the formerly closed lead after the compressed ice had consolidated enough to stay intact. The trailing edge of the semi-consolidated drift-ice matches the configuration of the fast-ice edge (Fig. 20). Thus, wind incidents of several-day duration have great influence on ice formation, movements and drift patterns. Rhythmical changes of local winds probably are mainly responsible for Laptev Sea flaw lead opening, closing and oscillations.

Fig. 20: Landsat image from April 9, 1992 shows trailing of the semi-consolidated drift ice (arrow in the zone of open water). The polynya west of Kotelnyy Island has a width of 10-15 km.

Dominance of northeastern and occasional strong southeastern and northwestern winds at Kotelnyy region during April 1992 are believed to have short range influence on local ice drift patterns in the northeastern area of investigation, seaward of the flaw lead (Fig. 21).

An average southwestward drift rate of 8 cm/s (0.15 knots) was measured by GPS readings for a large floe at Ref. No.14 (Fig. 3) on April 17 over a 7-hr period, at the beginning of 7 days of strong northeastern winds. Thus, large ice sheets could be transported during this period for a distance of 50-100 km to southwestern directions (Fig. 21). April 1992 Kotelnyy meteorological data (Fig. 8) differ from the recorded 34 year (1936-1970) mean for April (DIRGUNOVA et al. 1983), which show mainly southeastern wind directions. According to wind data and GPS readings the local ice drift movements during April this year are partially distinct from presumed Laptev Sea ice drift during April to June after GUBKOVICH et al. (1983) (Fig. 21). Due to this year (short range) observations the conclusion can be made, that Laptev Sea local pattern of drift ice movements are probably much more complex than commonly shown in generalized ice maps.

6.2 Sediment entrainment

Wind as a potential transport agent for terrigeneous material onto the Arctic sea ice cover has been discussed repeatedly (ARNOLD 1961; CLARK & NOONE 1985; KINDL 1924; RAHN 1982; REIMNITZ & MAURER 1979). Especially, PFIRMAN et al. (1989a) speculate that it might be important for the Siberian shelf areas. Our measurements in snow, however, indicate that eolian sediment transport is insignificant for the sedimentary budget of Laptev Sea ice. The overall particle concentrations in snow are low compared to those in sea ice. Moreover, the expected higher concentrations in the proximity of windward coasts and an offshore decrease in sediment content could not be observed. Except in the very restricted environment of the Lena River (Ref. No. 2 in Fig. 3), where clear discoloration of the snow cover was very noticeable even from the air, long-range eolian transport is insignificant.

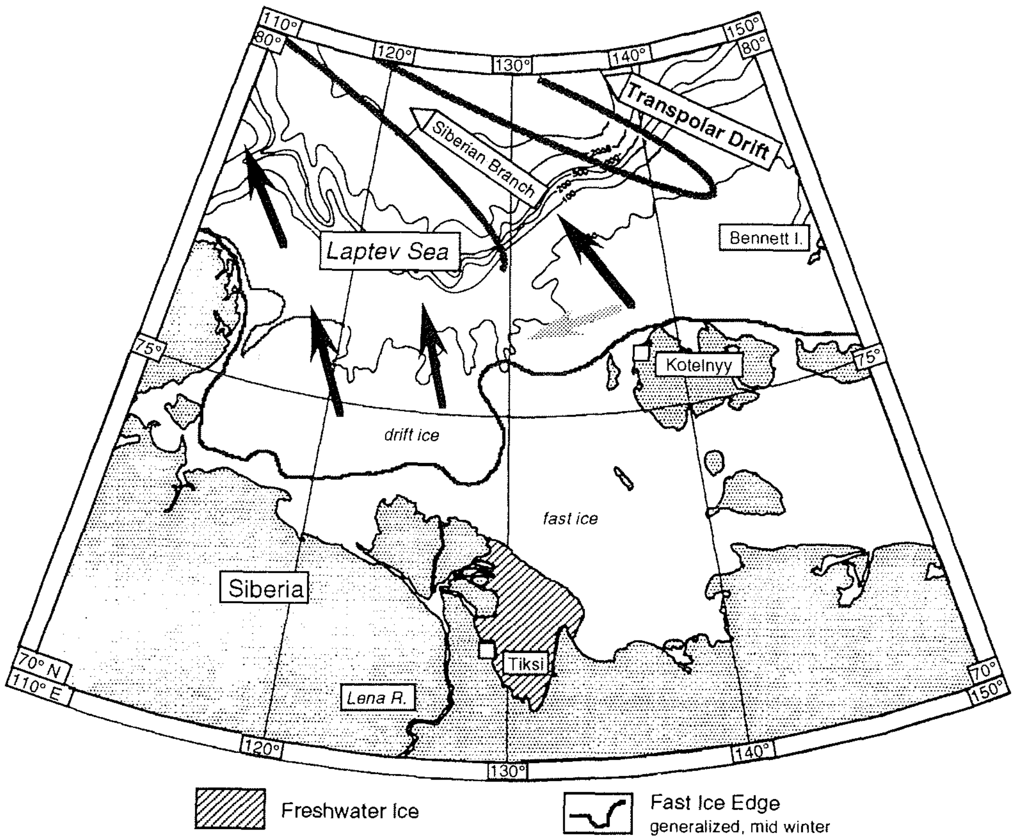

Fig. 21: Local ice drift in the northeastern study area (grey arrow) as indicated from meteorological data and GPS readings for parts of April 1992. Black arrows indicate presumed general ice drift directions during period from April to June (after GUBKOVICH et al. 1983).

Our observations indicate that sediment entrainment by suspension freezing is not active during the period from February to May in the Laptev Sea. Prograding of the fast ice from shallow coastal areas to the 20-30 m isobath occurs during the cold period between November and January (Fig. 12). Shallow shelf areas and wind induced turbulence of supercooled water are thought to promote the mechanism and incorporation of sediment and thus different chemical pollutants. The extensive shallows were covered by ice at the time of field observations. We suspect that large loads are exported from the Laptev Sea during fall, and that such dirty ice might be recognized as a seasonal signal in the Transpolar Drift during winter or next spring. In accordance with the hypothezised high fall entrainment rates in Siberian source areas, amounts of sediment released from melting sea ice in ablation areas would fluctuate rhythmically. After unfavorable autumn sediment-entrainment conditions, deposition in ablation areas could be reduced or stopped for several years. Such variations in sediment flux are suggested by very low loads observed in Fram Strait from June 15 to July 3, 1990 and very high loads a month later (pers. com. Erk Reimnitz, May 1992).

Knowledge of modern sea-ice formation, sediment entrainment, transport, and ablation should eventually lead toward a better understanding of fluctuations in Arctic Ocean deposition patterns during Quaternary glacial/interglacial cycles. With a sea level temporary more than 120 m below that of the present during the late Pleistocene glacial maximum 18.000 y. B.P. (BARD et al. 1988), the present wide Arctic shelf shallows were dry. Most areas of the recent Laptev Sea were covered by alluvial and loess-ice plains. In some parts of the eastern Arctic the submerged shoreline was located at the level of the present day 100 m isobath at that time (BIRYUKOV et al. 1988). Thus, modern mechanisms of sea ice sediment entrainment would not be very effective during these periods, because they heavily depend on the extent of shallow water regions. Also, temporary absence or areal reduction of the East Siberian polynya "ice factories" in the geological past might have had great influence on ice production rates for the entire Arctic Ocean and thus a redundant effect on global climate processes. Due to the worldwide postglacial transgression the water-covered shallows in the eastern Arctic progressively assumed the modern extent. However, in accordance to paleogeographic maps (HOLMES & CREAGER 1974), the polynya ice formation- and sediment entrainment processes could have been recommenced at the very earliest 15,000 y. B.P., but most likely not until 11,500 y. B.P. ZAKHAROV (1966) estimated a recent ice production rate of 910 km^3 in the Laptev Sea flaw leads alone during the coldest period from October to April. A similar ice volume is produced over the rest of the shelf. Thus, through the loss of the Laptev sea as an ice production area alone, the new-ice budget of the Arctic Ocean would be reduced by well over 1000 km^3/yr during cold geological periods. Sea-ice extent, ablation rates and certainly the related sediment transport and deposition rates probably could have been much smaller for the entire Arctic Ocean than today.

6.3 Indications for different source areas

Our investigation of sediment load in the ice of the Laptev Sea and that northward thereof shows that it has different source areas. The patches of dirty ice within the fast ice area probably originated from areas shallower than 20 m within the Laptev Sea during fall. Dirty drift ice sampled north of the New Siberian Islands and off Bennett Island probably originated from sources to the east, perhaps as far away as the Chukchi Sea, following the Transpolar Drift. Future analyses of clay minerals, and of anthropogenic pollutants should ascertain this belief. Ice produced in the Laptev Sea polynya in January to May provides only little, if any sediment to the Transpolar Drift. Any sediment contained would probably originate from 20-30 m water depths.

6.4 Freshwater influence on suspension freezing processes

Multi-year ice was only seen north- and northeastward of the New Siberian Islands, but not in the Laptev Sea itself. This sea therefore was completely ice free prior to the freezeup of 1991, and the ice observed and sampled records events of one winter only. A 100-km wide region of continuous to patchy fresh-water ice along the eastern delta flank is a striking feature, when compared to coastal ice of Arctic Alaska. Discharge of northern Alaska's small rivers is greatly reduced or terminated at the time of freeze-up at sea, and therefore the shallow coastal waters are mixed to the bottom at salinities of 32 ppt during freeze-up storms, following summer salinities of 20-25 ppt (REIMNITZ et al. 1987). The fresh-water ice seen far seaward off the Lena River indicates that river discharge here dominated the hydrography well into freeze-up. Surface water salinities at Ref. Nos. 4, 5, and 6 of 0.0, 14.0, and 11.0 ppt, respectively, show the lasting influence of the river even in April, when there should be no actual discharge (Fig. 5).

ZAKHAROV (1966) wrote that in the Laptev Sea flaw lead the freshening by large rivers stabilize the water column so firmly that convection can not exceed 22 m. However, in most areas this is "quite sufficient for convection to extend to the bottom", and this convection aerates bottom waters and promotes benthic life. This would imply that the formation of frazil and its accretion on the sea floor as anchor ice could occur in mid winter in some areas below the polynya. The apparent absence of sediment-laden new ice seaward of the lead, and the low particle flux seen in the trap deployed in the lead, on the other hand, suggests that suspension freezing does not extend to the bottom in mid winter.

Laboratory experiments showed that the formation of anchor ice is greatly facilitated when bottom sediments are ice bonded, or when the interstitial water is frozen (KEMPEMA et al. 1986). This occurs when summer waters of low salinity, which also diffuse into surface sediments, are replaced by waters of higher salinity during the onset of winter. The relatively low salinities within sediments are preserved for some time after river discharge ceases by the slow rates of molecular diffusion of seawater salts back into the sediment (REIMNITZ et al. 1987). This salinity lag in bottom sediments results in ice bonding, when more saline sea waters at their lower freezing temperature sweep across the bottom. Freezing point differences across the water/sediment interface should be much greater off this large river, and therefore the formation of anchor ice more prevalent. Strong evidence for the action of anchor ice, in form of small patches of delicately structured sediment inclusions, was seen not only in fresh-water ice around the delta, but also in turbid sea ice. As nothing is known about these phenomena and the bottom-water conditions in the Laptev Sea, they must be studied in the future.

7. CONCLUSIONS

The most important results of E.S.A.R.E. '92 are summarized as follows:

1) A zone of large grounded pressure ridges (stamukhi) stabilizing the fast ice on the Arctic shelf of North American is not seen along the edge of the fast ice in the Laptev Sea. Its absence reflects a lack of onshore ice pressure.
2) A 10 to 15-km wide, recurring flaw lead (polynya) instead borders the edge of the smooth fast ice, and is maintained by dominantly offshore winds.
3) A large volume of freshwater discharged by the Lena River and its eastward deflection is recorded in a 100-km wide region of freshwater ice, with a slick surface largely bare of snow, east of the delta.
4) During the period from January through April the lead lies at water depths ranging from 20 to 30 m, with the configuration of the fast ice edge at least locally controlled by shoals.
5) Large amounts of ice are produced in the polynya, which totally surrounds the Laptev Sea for a distance of nearly 1800 km.
6) During the period of our study, only first-year ice occurred in the Laptev Sea, indicating that the sea was totally ice free during late summer of the previous year.
7) The ice produced seaward of 20 m and continuously advected offshore was clean in April. We believe that a water column firmly stratified from river water input may prevent effective sediment entrainment during late winter.
8) Conditions for sediment entrainment may be optimal during freeze-up, when vast shallow regions are exposed to fall storms. Continuous ice export, with a short period of entrainment followed by a long period of clean ice production would cause large and rythmical variations in sediment flux out of the Laptev Sea.
9) The occurrence of delicately structured sediment inclusions and of turbid ice within the fast ice, indicate that anchor- and frazil ice were principal entrainment mechanisms.
10) Wind transport from land to sea must be ruled out as important for the occurrence of fine particulate matter in pack ice of the Transpolar Drift.
11) The ice drifting westward past the Laptev Sea carries large amounts of sediment compared to that advected from this sea during winter.
12) The yearly occurrence of the flaw lead is a function of present atmospheric pressure patterns. Rates of ice production, release of cold brines, and sediment flux from the Laptev Sea probably varied during the postglacial rise of sea level, and will vary with any climatic change.
13) Short periods of strong wind incidents have great influence on ice formation, polynya opening, closing and oscillation and the patterns of drift ice movement.
14) The vertical particulate flux at 10 m depth was high at a site with a total water depth of 17.5 m in May 1991 and very low at a site with a total water depth of 28 m in April 1992. This indicates a different resuspension rate. The results are in a good agreement with ZAKHAROV (1966) who estimated the vertical convection in Laptev Sea flaw leads reaching 22 m as a maximum.

8. ACKNOWLEDGEMENTS

Naming all the persons involved in making this study possible can not be done in this context, but they certainly are not too many for us to remember fondly. We are indebted to Prof. Jörn Thiede for his great support of Arctic sea-ice research. Dr. Heidemarie Kassens has been a inalienable helping hand in GEOMAR preparations for the expedition. We also mention Dr. Sergey M. Pryamikov of AARI, who was in overall charge of the difficult logistics and the many arrangements. The helicopter crew, especially the pilots, earned our highest respect and trust, and we thank them. We also are greatful to William Shatohin, the chief of the small navigation station at Kotelnyy, for his wonderful hospitality and authentic foods he prepared. Research funds were provided by the Bundesministerium für Forschung und Technologie (BMFT), by the Deutsche Forschungsgemeinschaft (DFG), by DFG-Leibniz TH 200/5-1 and by U.S. ONR contract No. N 00014 - 88- J -1087.

9. REFERENCES

Aagaard, K., Swift, J.H. & Carmack, E.C. (1985): Thermohaline circulation in the Arctic Mediterranean Seas. - J. Geophys. Res., 90 (C5), 4833-4846.

Arnold, K.L. (1961): An investigation into methods of accelerating the melting of snow by artificial dusting. - Geol. Arctic, 989-1013.

Bard, E., Hamelin, B., Fairbanks, R. G. & Zindler, A. (1990): Calibration of the ^{14}C timescale over the past 30,000 years using mass spectrometric U-Th ages from Barbados corals. - Nature, 345, 405-410.

Barnes, P.W., Reimnitz, E. & Fox, D. (1982): Ice rafting of fine-grained sediment, a sorting and transport mechanism, Beaufort Sea, Alaska.- J. Sed. Pet., 52 (2), 493-502.

Barnett, D. (1991): Sea ice distribution in the Soviet Arctic. - In L.A.Brigham (ed.): The Soviet Maritime Arctic, Belhaven Press, London, 47-62.

Biryukov, V. Y., Faustova, M. A., Kaplin, P. A., Pavlidis, Y. A., Romanova, E. A. & Velichko, A. A. (1988): The paleogeography of Arctic shelf and coastal zone of Eurasia at the time of the last glaciation (18,000 yr B.P.). - Palaeogeogr., Palaeoclimat., Palaeoecol., 68, 117-125.

Cattle, H. (1985): Diverting Soviet rivers: Some possible repercussions for the Arctic Ocean. - Polar Record, 22 (140), 458-498.

Clark, D.L. (1990): Arctic ocean ice cover; geologic history and climatic significance. - In A. Grantz, L. Johnson & J.F. Sweeney (eds.): The Arctic Ocean Region, Geol. Soc. Am., The Geology of North America, L, Boulder, Colorado, 53-62.

Clark, D.L. & Noone, K.J. (1985): Soot in the Arctic icepack: A cause for pertubations in radiative transfer. - Atmosph. Environm., 19/12, 2045-2053.

Colony, R. & Thorndike, A.S. (1985): Sea ice motion as a drunkard's walk. - J. Geophys. Res., 90 (C1), 965-974.

Dirgunova, E.N., Uchanova, E.V. & Savialova, I.N. (1983): Map of Arctic Ocean near surface winds. - In S. G. Gorshkov (ed.): World Ocean Atlas, Vol. 3, Arctic Ocean, 86-87.

Fuchs, V.E. & Whittard, W.F. (1930): The East Greenland pack-ice and the significance of its derived shells. - Geograph. J., 76, 419-424.

Geological Society of America (1986): Bathymetry of the Arctic Ocean. - Map and Chart Series MC 56, Boulder, Colorado.

Gierloff-Emden, H.G. (1982): Das Eis des Meeres. - Walter de Gruyter, Berlin, 767-940.
Gordienko, P.A. & Laktionov, A.F. (1969) Circulation and physics of the Arctic Basin waters. - Ann. Internat. Geophys. Year, Oceanogr., Pergamon, New York, 46, 94-112.
Gubkovich, S. M., Nikolayeva, A. J. & Volkov, N. A. (1983): Map of Arctic ice drift. - In S. G. Gorshkov (ed.): World Ocean Atlas, Vol. 3, Arctic Ocean, 145-147.
Holmes, M.L. & Creager, J.S. (1974): Holocene history of the Laptev Sea continental shelf. - In Y. Herman (ed.): Marine Geology and Oceanography of the Arctic Seas, Chapter 9, Springer Verlag, Berlin, 211-229.
Kempema, E.W., Reimnitz, E. & Hunter, R.E. (1986): Flume studies and field observations of the interaction of frazil and anchor ice with sediment. - U. S. Geol. Surv. Open-File Rep., 86-515, 48 pp.
Kempema, E.W., Reimnitz, E. & Barnes, P.W. (1989): Sea ice sediment entrainment and rafting in the Arctic. - J. Sed. Pet., 59 (2), 308-317.
Kerr, R.A. (1992): U.S. - Russian Team Solves Arctic Mystery. - Science, 257, 35.
Kienle, J., Roederer, J.G. & Shaw, G.E. (1983): Volcanic event in the Soviet Arctic? - EOS 64 (20), 377-380.
Kindle, E.M. (1924): Observations on ice-borne sediments by the Canadian and other arctic expeditions. - Am. J. Sci., 5th Series, 7 (40) 249-286.
Klyuyev, Ye. V. (1965): The role of permafrost factors in the dynamics of bottom topography in polar sea. - Oceanol., Acad. Sci. U.S.S.R., 5 (1), 78-83.
Klyuyev, Ye.V. & Kotyukh, A.A. (1985): Some peculiarities of the dynamics of the relief on the bed of the Laptev Sea, Leningrad State University. - Polar Geogr. Geol., 9 (4), 301-307.
Ledley, T.S. & Thomson, S.L. (1986): Potential effect of nuclear war smokefall on sea ice. - Climat. Change, 8, 155-171.
Martin, S. & Cavalieri, D.J. (1989): Contributions of the Siberian shelf polynyas to the Arctic Ocean intermediate and deep water. - J. Geophys. Res., 94 (C9), 12,725-12,738.
Melnikov, S. A. & Vlasov, S. V. (1990): A summary report on contaminant levels in the compartments of the marine environment of the Arctic Seas in 1990. - unpubl. Rep., Arctic and Antarctic Research Institute, St. Petersburg, Russia, CIS.
Milliman, J.D. & Meade, R.H. (1983): World-wide delivery of river sediment to the oceans. - J. Geol., 91, 1-21.
Mysak, L.A. & Manak, D.K. (1989): Arctic sea ice extent and anomalies, 1953-1984. - Atmosphere Ocean, 27 (2), 376-405.
Nürnberg, D. (1992): Sediment inclusions in the sea ice. - In D. Fütterer & Shipboard Scientific Party, Arctic '91: The expedition ARK VIII/3 of RV "Polarstern" in 1991, Ber. Polarforsch.,107 (1992), 29-33.
Pfirman, S.L., Wollenburg, I., Thiede, J. & Lange, M.A. (1989a): Lithogenic sediment on Arctic pack ice - Potential aeolian flux and contribution to deep sea sediment. - In M. Leinen & M. Sarnthein (eds.): Contribution to the NATO Advanced Workshop; Paleoclimatology and Paleometeorology: Modern and past patterns of global atmospheric transport, NATO ASI Series C, 282, 463-491.
Pfirman, S.L., Gascard, J.-C., Wollenburg, I., Mudie, P. & Abelmann, A. (1989b): Particle-laden Eurasian Arctic sea-ice: observations from July and August 1987. - Polar Res., 7, 59-66.
Rahn, K.A. (1982): On the causes, characteristics and potential environmental effects of aerosol in the Arctic atmosphere. - in review, 163-195.

Reimnitz, E., Toimil, L.J. & Barnes, P.W. (1978): Arctic continental shelf morphology related to sea-ice zonation, Beaufort Sea, Alaska. - Mar. Geol., 28, 179-210.
Reimnitz, E. & Maurer, D.K. (1979): Eolian sand deflation - A cause for gravel barrier islands in arctic Alaska? - Geology, 7 (10), 507-510.
Reimnitz, E. & Kempema, E.W. (1984): Pack ice interaction with Stamukhi Shoal, Beaufort Sea, Alaska. - In P.W. Barnes, D.M. Schell & E. Reimnitz (eds.): The Alaskan Beaufort Sea, Ecosystems and Environment, Academic Press, Orlando, Florida, 159-184.
Reimnitz, E. Kempema, E.W. & Barnes, P.W. (1987a): Anchor ice, seabed freezing, and sediment dynamics in shallow arctic seas. - J. Geophys. Res., 92 (C13), 14,671-14,678.
Reimnitz, E. & Barnes, W.P. (1987b): Sea-ice influence on Arctic coastal retreat. - In N.C. Kraus (ed.): Coastal Sediments '87, Proceedings of a Speciality Conference on Advances in Understanding of Coastal Sediment Process, New Orleans, Vol. 2, 1578-1591.
Reimnitz, E. & Saarso, M. (1991): Studies of Sediment Transport by Ice. - In J. Thiede & G. Hempel (eds.): Die Expedition Arktis VII-I, mit FS "Polarstern" 1990, Ber. Polarforsch. 80, 44-50.
Reimnitz, E., Marincovich, L., Jr., McCormick, M. & Briggs, W.M. (1992): Suspension freezing of bottom sediment and biota in the Northwest Passage and implications for Arctic Ocean sedimentation, Canad. J. Earth Sci., 29, 693-703.
Reimnitz, E., Clayton, W.S., Jr., Kempema, E.W., Payne, J.R. & Weber, W.S. (in press b): Interaction of rising frazil with suspended particles in tank experiments. - Cold Regions Science and Technology, 1992.
Smith, S.D., Muench, R.D. & Pease, C.H. (1990): Polynyas and leads: An overview of physical Processes and Environment. - J. Geophys. Res., 95 (C6), 9461-9479.
Tomirdiaro, S.V. (1975): Thermo abrasion-induced shelf formation in the eastern arctic seas of the USSR during the Holocene. - Earth Sci. Sec., 219 (1-6), 23-26.
Untersteiner, P. (1990): Structure and dynamics of the Arctic Ocean ice cover. - In A. Grant, L. Johnson & J.F. Sweeney (eds.): The Geology of North America; The Arctic Ocean Region. Geol. Soc. Am., Boulder, Colorado, 37-52.
Wollenburg, I. (1991): Sedimentransport durch das arktische Meereis - Die rezente lithogene und biogene Materialfracht. - Math.-Naturwiss. Fakult. Christian-Albrechts-Universität Kiel, unpublished Ph.D. thesis, 187 pp.
Zakharov, V.F. (1966): The role of flaw leads off the edge of fast ice in the hydrological and ice regime of the Laptev Sea. - Academy of Sciences of the USSR, Oceanology, 6 (1), 815-821.
Zakharov, V.F. (1976): Cooling of the Arctic and the ice cover of the Arctic Seas (translation from Russian by the Norsk Polarinstitutt). - AANII, Trudy, 37, 96 pp.
Zenkovitch, V.P. (1985): Arctic USSR. - In E.C.F. Bird & M.L. Schwarz (eds.): The World's Coastline. Van Nostrand Reinhold Company, New York, 863-871.

10. APPENDIX

Table 1: List of stations

Date	Jul. Date - Station	Ref. No.	Latitude	Longitude
06.04.1992	97-1	1	71° 45´ N	128° 45´ E
	97-2	1	71° 45´ N	128° 45´ E
07.04.1992	98-1	2	71° 45´ N	127° 09´ E
09.04.1992	100-1	4	72° 30´ N	130° 00´ E
09.04.1992	100-2	5	73° 29´ N	129° 58´ E
10.04.1992	101-1	6	73° 45´ N	128° 15´ E
11.04.1992	102-1	7	74° 06´ N	125° 01´ E
11.04.1992	102-2	8	74° 29´ N	129° 50´ E
12.04.1992	103-1	3	71° 48´ N	129° 00´ E
16.04.1992	107-1	13	75° 59´ N	137° 53´ E
17.04.1992	108-1	14	76° 59´ N	134° 58´ E
17.04.1992	108-2	11	76° 00´ N	133° 05´ E
20.04.1992	111-1	17	79° 00´ N	140° 01´ E
21.04.1992	112-1	12	75° 49´ N	135° 26´ E
21.04.1992	112-2	15	77° 48´ N	140° 04´ E
21.04.1992	112-3	16	77° 29´ N	133° 11´ E
22.04.1992	113-1	10	75° 29´ N	132° 12´ E
22.04.1992	113-2	9	74° 11´ N	130° 28´ E
23.04.1992	114-1	18	77 44´ N	140° 21´ E

Table 2: List of samples

Date	Jul. Date-Stat.	Latitude	Longitude	Sample	Comments
06. 04.1992	97-1	71° 45´ N	128° 45´ E	Stones	Hill behind Tiksi town
06. 04.1992	97-2	71° 45´ N	128° 45´ E	Sand	Tiksi beach sand
07. 04.1992	98-1	71° 45´ N	127° 09´ E		
07. 04.1992	98-1-1			Ice	Sample 1 (first landing) Laser Gs TTU
				Ice	No. 2 grain size sample
				Ice surface	Lena-River
				River ice core	Lena 0-10 cm (Pf)
				Ice core	0-40 cm
				Ice core	41-90 cm, exclusive 47-55 cm
				Ice core	90-130 cm
				River ice core	Lena 47-55 cm (Pf)
				Snow	Lena River (Pf)
				Stone	From east beach Lena-River
				Ice	No. 2 grain size sample Laser Gs TTU
				Ice	No. 3 sample Laser Gs TTU
				Ice core	130 cm (SM)
				Geological	E Bank (Lena-River)
07. 04.1992	98-1-2			Stones	Stones from beach Lena-River
				Sand	From beach (W) Lena-River
				Ice	Laser Gs TTU
				Sand	From beach (W) Lena-River

Date	Jul. Date-Stat.	Latitude	Longitude	Sample	Comments
09. 04.1992	100-1	72° 30´ N	130° 00´ E	Snow	(Pf)
				Ice	Laser Gs TTU
				Snow	A with Alc. (Ab)
09. 04.1992	100-1-1			Ads. Column	Org. pollution enriched from sea water
				Filtered SPM	1 (one) filter used
				Ice	Sample 100 cm (SM)
				Ice core	Ice core from 34-47 cm (Pf)
				Bottom sed.	Bottom sediment from sub ice corer
09. 04.1992	100-1-2			Sediment rest	Sediment rest. from sub ice corer
				Water	Sample (SM)
				Ice core	81-160 cm + 103-1-1 mitte
09. 04.1992	100-1-3			Ice core	Mixed + 103-1-1 unten
				Ice core	0-80 cm + 103-1-1 (oben)
				Water	Lena delta 17.5 m water depht. Bailed out of ice hole,
09. 04.1992	100-2	73° 29,7´ N	129° 58,09´ E	Water	160 cm deep 14 ppm sal. probably high. (Pf) ∂O18
				Bottom sed.	Bottom sed. from sub ice corer
				Snow	(Pf)
				Bottom sed.	Bottom sed. from sub ice corer (rest)
				Ice core	Ice core bottom and sea water, sal. 0 0/00 (Gr)
				Bottom	Laser Gs, TTU
				Ice	Laser Gs, TTU
09. 04.1992	100-2-2			Ice core	0-60 cm
				Ice core	61-120 cm
				Ice core	121-178 cm
				Water	Sample + slush
10. 04.1992	101-1	73° 44,6´ N	128° 14,9´ E	Ice	Just bottom ice 11.5 ppm (PF) ∂18 0
				Snow	Sample melted in microwave (Pf)
				Snow	(Gr)
				Snow	With Alcohol (Ab)
				Water	Water for ∂18 O (Pf)
10. 04.1992	101-1-2			Bottom sed.	Bottom sed. from sub ice corer (ca. 12 cm)
				Ice core	0-78 cm
				Ice core	0-78 cm
				Ice core	0-78 cm
				Ice core	Ice core bottom and sea water; 14,5 o/oo in ice hole (Gr)
				Water a. slush	SM
				Ice core	SM
11. 04.1992	102-1	74° 05,6´ N	125° 01´ E	Snow	A biol. 4% Alc. (Ab)
				Ice core	30-55 cm Laser Gs TTU, turbid layer from ice core
				Bottom sed.	B bottom Laser Gs TTU
				Snow	A biol.
11. 04.1992	102-1-2			Ice core	152-156 cm, bottom of ice core and filtered sea water (Gr)
				Snow	Snow for ∂18 O (Pf)
				Bottom sed.	Bottom sed. from sub ice corer
11. 04.1992	102-1-3			Ice core	SM
				Water a. slush	SM
				Ice core	150-155 cm, ice core bottom and filtered sea water (Gr)
				Ice core	0-50 cm
				Ice core	51-100 cm
				Ice core	101-150 cm
11. 04.1992	102-2	74° 28,7´ N	129° 49,5´ E	Bottom	Laser Gs, TTU
				Snow	A biol. 4% Alc.
				Snow	Snow for ∂18 O (Pf)
11. 04.1992	102-2-1			Bottom sed.	Sub ice corer (ca. 10 cm)
				Ice core	86-90 cm, ice core bottom and filtered sea water, (GR)
				Snow	A with Alc. (Ab)
11. 04.1992	102-2-2			Bottom sed.	Taken from sub ice corer
				Bottom sed.	Taken from sub ice corer
				Bottom sed.	Taken from sub ice corer
				Bottom sed.	Taken from sub ice corer
				Ice core	90 cm length and 113-2-2 (66-135 cm)
11. 04.1992	102-2-3			Ice core	90 cm length and 113-2-2 (0-65 cm)
11. 04.1992	102-2-4			Ice core	SM
				Water	SM
				Ice core	90 cm length and 113-2-2, (136-180 cm) + 113-2-3, 20 cm lengtl
12. 04.1992	103-1	71° 48,5´ N	129° 00,0´ E	Ice core	Sed. 2-3 cm depht
				Ice core	Ice core 20-30 cm (Pf)
				Water	Water for Tritium (Pf)
12. 04.1992	103-1-1			Ads. Column	Org. pollution enriched from sea water
				Filtered SPM	3 (three) filters used
				Ice core	Upper and 100-1-3, 0-80 cm

Date	Jul. Date-Stat.	Latitude	Longitude	Sample	Comments
12. 04.1992	103-1-1	71° 48,5´ N	129° 00,0´ E	Ice core	Middle and 100-1-3, 81-160 cm
				Ice core	Lower and 100-1-3, mixed
				Water	Water for ∂18 O (Pf)
				Snow	A Snow for ∂18 O (Pf)
				Water	Sample (SM)
				Ice core	SM
				Bottom sed.	From sub ice corer
				Snow	A with Alc. (Gr)
				Snow	Snow with Alc. (Ab)
12. 04.1992	103-1	71° 45´ N	128° 45´ E	Fishes	Ref. meas. PCB, Bay of Tiksi
16. 04.1992	107-1	75° 59,5´ N	137° 53,1´ E	Snow	Laser Gs, TTU dusty snow on the coast line near Kotelnyy Statio
				Ice	Laser Gs, TTU
17. 04.1992	108-1	76° 59,3´ N	134° 58,3 ´E	Snow	A biol. 4% Alc. (Gr)
				Snow	A biolog. 4 % Alc. (Ab)
				Bottom	B Laser Gs TTU
				Water	Sub ice water for Tritium (Pf)
				Ice	No. 2 Laser Gs, TTU
				Ice	No. 1 Laser Gs, TTU
17. 04.1992	108-1-1			Ice core	0-90 cm, and 112-3-2, 121-180 cm
17. 04.1992	(108-1-1/2)			Ice core	Mixed, and 112-3-2 (61-120 cm)
17. 04.1992	(108-1-2/3)			Ice core	Mixed, and 112-3-2 (0-60 cm)
				Ads. Column	Org. pollution enriched from sea water
				Filtered SPM	1 (one) filter used
				Ice core	135-138 cm, ice core bottom, 4% Alc., (Gr)
17. 04.1992	108-1-2			Water a. slush	SM
				Ice core	0-90 cm, and 112-3-2 (0-60 cm)
				Ice	SM
17. 04.1992	108-1-4			Bottom sed.	Snapper
				Seafloor sed.	No
				Seafloor sed.	No
				Seafloor sed.	No
17. 04.1992	108-2	76° 00´N	133° 05,1´ E	Seafloor sed.	With large stone
				Bottom	No
				Seafloor	Bottom sample through seal hole, with cucumber
				Bottom	Laser Gs, TTU
				Snow	A biol., 4% Alc. (Ab)
				Snow	A biol., 4% Alc., (Gr)
17. 04.1992	108-2-1			Water	SM
				Ice	SM
				Bottom sed.	Lead line, taken from weight
				Ice core	94-97 cm, ice core bottom, 4 % Alc., (Gr)
17. 04.1992	108-2-3			Bottom sed.	Grap. bottom sediment, surface
				Bottom sed.	Grap. bottom sediment, surface
				Seafloor sed.	No
17. 04.1992	108-2-4			Ice core	0-98 cm and 113-1-2, 141-210 cm
17. 04.1992	108-2-5			Ice core	0-98 cm and 113-1-2, 0-71 cm
17. 04.1992	108-2-6			Ice core	0-98 cm and 113-1-2, 71-140 cm
20. 04.1992	111-1	79° 00,9´ N	140° 01,261´ E	Water	Sub ice water for Tritium (Pf)
				Snow	Snow for (Pf)
				Dirty ice	Turbid
				Water	Sub ice water for ∂18 O (Pf)
				Ice	No. 1 Laser Gs, TTU, turbid ice from pressure ridge
				Ice	No. 3 Laser Gs, TTU, thin turbid layer in ridges
				Ice	No. 4 Laser Gs, TTU, very turbid granular ice
				Ice	No. 5 Laser Gs, TTU, sediment layer on one side of ice block
				Turbid ice	Core from turbid ice
				Meltwater	From 5 jars combined Mart, thinks ER´s, stat.
20. 04.1992	111-1-1			Snow	A, 4% Alc. (Gr)
				Snow	A, 4% Alc. (Ab)
				Water a. slush	SM
				Ice	SM
				Ice core	0-80 cm, and 112-2-2 (0-80 cm)
				Ice core	81-170 cm, and 112-2-3 (0-30 cm + 90-123 cm)
				Ads. Column	Org. pollution enriched from sea water
				Filtered SPM	1 (one) filter used
				Water	Sub ice water (Pf) ∂18 O
20. 04.1992	111-1-2			Ice	Conc. 1, TTU
				Ice	Conc. 2, TTU
				Ice core	72-175 cm, Laser Gs, TTU
				Ice core	Mixed and 112-2-2 81-123 cm
20. 04.1992	111-1-4			Ice core	2 cm, 170 cm core in filtered seawater 20 µm, 4 % Alc. (Gr)

Date	Jul. Date-Stat.	Latitude	Longitude	Sample	Comments
20. 04.1992	111-1-6/111-1-7	79° 00,9´ N	140° 01,261´ E	Ice cores	Two combined ice cores for ∂18 O (Pf)
				Ice cores	Two ice cores
21. 04.1992	112-1	75° 49´ N	135°26,8´ E	Bottom	Laser Gs (ST site), TTU
				Sediment	Sediment trap sample, TTU
				Water	Surface and bottom salinity
21. 04.1992	112-1-1	75° 49´ N	135°26,8´ E	Seafloor sed.	No
				Bottom surf.	Snapper
21. 04.1992	112-2	77° 48´N	140° 04´ E	Seafloor sed.	Snapper
				Bottom surf.	Snapper
				Snow	Snow A for biology, 4 % Alc. (Ab)
				Bottom	Laser Gs, TTU
				Bottom	Laser Gs, TTU
				Snow	Snow for biology, 4% Alc., (Gr)
				Seafloor sed.	60 m depth
21.04.1992	112-2-1			Ice core	In seawater (120-123 cm), (Gr)
21. 04.1992	112-2-2			Ice core	0-80 cm, and 111-1-1 (0-80 cm)
				Water	SM
				Ice	SM
				Ice core	81-123 cm and 111-1-2 mix
21. 04.1992	112-2-3			Ice core	0-30 cm/90-123 cm, and 111-1-1 (81-170 cm)
21. 04.1992	112-3	77 ° 29,3´ N	133° 11,7´ E	Snow	A biol. 4% Alc. (Gr)
				Ice Core	0-75 cm, Laser Gs, TTU
				Ice Core	Laser Gs, TTU
				Snow	A biol., 4% Alc.
				Bottom	Laser Gs, TTU
21. 04.1992	112-3			Bottom sed.	Snapper
		77° 29,3´ N	133° 11,7´ E	Bottom sed.	Snapper
21. 04.1992	112-3-1			Ice core	234-237 cm, ice core bottom in sea water, 4% Alc., (Gr)
				Water	SM
21. 04.1992	112-3-2			Ice core	0-60 cm and 108-1-2/3 mix
				Ice core	61-120 cm and 108-1-1/2 mix
				Ice core	121-180 cm and 108-1-1, 0-90 cm
				Ice	SM
21. 04.1992	112-3-3			Seafloor sed.	No
22. 04.1992	113-1	75° 29,2´ N	132° 12,9´ E	Sediment	Selected from anchor ice inclusions
				Snow	A biol.
				Snow	A biol.
				Ice	No. 2, Laser Gs, TTU
				Ice	No. 3, Laser Gs, TTU
				Ice	No. 4, Laser Gs, TTU
				Ice	No. 5, Laser Gs, TTU
				Dirty ice	Thin layer turbid
22. 04.1992	113-1-1			Ice core	Bottom and 4% Alc. (203-207 cm) (Gr)
22. 04.1992	113-1-2			Ice core	0-70 cm and 108-2-5, 0-98 cm
				Ice core	71-140 cm and 108-2-6, 0-98 cm
				Ice core	141-210 cm and 108-2-4, 0-98 cm
				Ice and slush	SM
				Ice	SM
				Ice	No. 1, Laser Gs, TTU
				Ads. Column	Org. pollution enriched from sea water
				Filtered SPM	3 (three) filters used
22. 04.1992	113-1-4			Ice	Anchor ice and org. material
22. 04.1992	113-2	74° 10,8´ N	130° 28,6´ E	Snow	Snow A (Gr)
22. 04.1992	113-2-1			Snow	Snow A biolg., 4 % Alc. (Ab)
				Ice core	Ice core bottom, 4 % Alc. (Gr)
				Ice core	0-55 cm, Laser Gs, TTU
				Ice core	66-135 cm, and 102-2-2 (90 cm)
22. 04.1992	113-2-2			Ice core	0-65 cm, and 102-2-3 (90 cm)
				Ice	SM
				Water	SM
				Ice core	136-180 cm, and 102-2-4 (90 cm), and 113-2-3, 20 cm lenght
22. 04.1992	113-2-3			Ice core	Length 20 cm, and 102-2-4 (90 cm), and 113-2-2 (136-180 cm)
23. 04.1992	114-1	77° 44,6´ N	140° 21,0´ E	Red ice	From Bennett Island, 4% Alc.
				Stones	NE coast Bennett Island
				Ice	No. 1, Laser Gs, TTU
				Ice	No. 1, Laser Gs, TTU
				Beach	No
23. 04.1992	114-1-7			Dirty ice	Turbid layer
23. 04.1992	114-1-8 (a)			Ice	Ice Ridge
				Ice	SM
23. 04.1992	114-1-8 (b)			Ice	Ice Ridge

Table 2: Abbreviations in Table 2

TTU:	Tallin Technical University
SPM:	Suspended particulate matter
SM	Heavy metals
GS:	Grain size analysis
SL:	Sea level
ST	Sediment trap
Pf:	Dr. Pfirman (Lamont-Doherty Geol. Obs., Palisades, USA)
Gr:	Dr. Gradinger (IPÖ, Kiel, FRG)
Ab:	Dr. Abelmann (AWI, Bremerhaven, FRG)
Jul. Date:	Julian Date
Stat.:	Station
Loc.:	Location at station

Table 3: Sediment load in snow samples of the study area. Data are presented in Fig. 16.

Sample #	Type of sample	Amount of water (ml)	Sediment per liter (mg/l)
981-1	snow A	355,00	197,17
981-1	snow B	295,00	107,24
981-1	snow C	315,00	202,92
100-1	snow A	352,00	49,76
100-1	snow B	376,00	14,25
100-1	snow C	430,00	4,20
100-2	snow A	959,00	2,60
100-2	snow B	330,00	1,55
100-2	snow C	380,00	12,86
101-1	snow A	248,00	2,44
101-1	snow B	281,00	7,02
101-1	snow C	204,00	23,21
102-1	snow A	348,00	1,90
102-1	snow B	340,00	19,14
102-1	snow C	242,00	2,59
102-2	snow A	278,00	13,73
102-2	snow B	224,00	13,38
102-2	snow C	283,00	12,12
103-11	snow A	368,00	28,62
103-11	snow B	338,00	37,41
103-11	snow C	382,00	40,74
107-1	snow	402,00	33,73

Sample #	Type of sample	Amount of water (ml)	Sediment per liter (mg/l)
107-1	snow	508,00	29,86
108-1	snow A	347,00	10,27
108-1	snow B	358,00	5,90
108-1	snow C	388,00	2,41
108-2	snow B	430,00	6,39
108-2	snow C	366,00	27,85
108-22	snow A	503,00	41,71
111-11	snow A	217,00	3,04
111-11	snow B	228,00	3,68
111-11	snow C	228,00	7,40
112-2	snow A	267,00	36,56
112-2	snow B	254,00	19,84
112-2	snow C	310,00	32,95
112-3	snow A	340,00	11,55
112-3	snow B	379,00	0,01
112-3	snow C	348,00	3,19
113-1	snow A	363,00	1,58
113-1	snow B	352,00	0,50
113-1	snow C	413,00	0,39
113-2	snow A	340,00	67,64
113-2	snow B	388,00	32,68
113-2	snow C	364,00	27,61

Table 4: Sediment load in ice samples of the study area. Data are presented in Fig. 17.

Sample #	Type of sample	Depth (cm)	Description	Amount of water (ml)	Sediment per liter (mg/l)
100-11	ice core	0-18		1156,00	30,19
100-12	ice core	0-21		1420,00	59,48
100-12	ice core	42-58		1148,00	2,00
100-12	ice core	73-90		1258,00	0,72
100-12	ice core	90-107		1191,00	0,39
100-12	ice core	107-117		657,00	1,66
100-12	ice core	117-145		1104,00	1,64
100-21	ice core	0-17		828,00	10,72
100-21	ice core	17-160		936,00	3,74
101-11	ice core	0-19		1246,00	1,39
101-11	ice core	57-75		972,00	1,11
102-11	ice core	40-52	Sed. layer	758,00	28,41
102-12	ice core	0-7		231,00	11,42
102-12	ice core	52-57		340,00	4,10
102-12	ice core	90-93		222,00	3,81
102-12	ice core	116-120		284,00	4,48
102-12	ice core	146-150		278,00	1,90
102-21	ice core	0-15	2 repr. chunks	730,00	2,27
102-21	ice core	72-86	2 repr. chunks	986,00	3,41
103-11	ice core	0-5		190,00	210,91
103-11	ice core		6 repr. pieces	965,00	2,32
108-12	ice core	0-6		450,00	2,61
108-12	ice core	42-48		443,00	1,07
108-12	ice core	72-78		502,00	2,05
108-12	ice core	120-126		403,00	2,64
108-13	turbid ice	surface		883,00	50,66
108-21	ice core	0-6		393,00	1,96
108-21	ice core	41-50		412,00	3,78
108-21	ice core	70-76		400,00	2,33
111-1-0	ice core		6 repr. pieces	1066,00	2,91
111-1-1	ice core		7 repr. pieces	734,00	1,60
111-1-1b	ice core		7 repr. pieces	1048,00	102,64
111-1-3a	ice core		6 repr. pieces	823,00	47,26
111-1-3b	ice core		6 repr. pieces	1020,00	156,03
111-1-4	ice core		6 repr. pieces	1286,00	0,92
111-1-5	ice core		6 repr. pieces	1140,00	1,48
111-1-6	ice core		6 repr. pieces	523,00	1,14
111-1-7	ice core		7 repr. pieces	720,00	57,33
111-1-8	ice core		7 repr. pieces	1256,00	55,84
111-1-9	ice core		7 repr. pieces	1123,00	10,42
111-1-12a	ice core		7 repr. pieces	322,00	52,96
111-1-12b	ice core		7 repr. pieces	1251,00	8,22
111-2	ice core			1170,00	4,21
112-2	turbid ice	surface		1950,00	132,41
112-31	ice core	001- 5		242,00	12,63
112-31	ice core	27-32		348,00	15,63
112-31	ice core	69-75		312,00	10,17
112-31	ice core	110-116		389,00	17,32
112-31	ice core	178-184		327,00	2,45
112-31	ice core	227-230		358,00	3,49
113-12	ice core	0-34		1128,00	98,02
113-13	anchor ice	24 cm below ice surface		1218,00	783,98
113-13	ice core	0-60	4 repr. chunks	1402,00	140,41
113-15	turbid ice	surface	4 repr. chunks	1168,00	272,20
113-16	ice core	0-30	turbid ice	1361,00	16,70
113-21	ice core			1348,00	6,82
114-1	red ice	surface	repr. chunks	520,00	160,75
114-12	turbid ice	surface	repr. chunks	788,00	255,52
114-13	turbid ice	surface	repr. chunks	678,00	184,74
114-14	turbid ice	surface	repr. chunks	832,00	963,67
114-14	turbid ice	see 1. filter	repr. chunks	832,00	276,22
114-15	turbid ice	surface	repr. chunks	708,00	3774,50
114-15b	turbid ice	surface	repr. chunks	708,00	492,53
114-16	turbid ice	surface	repr. chunks	782,00	328,11

Table 5: Grain size distribution and abundances of most important sediment components as estimated from smear slides.

Grain size analysis (Numbers in %)

Station-#	Ref.-#	Sand	Silt	Clay	Sediment type
9811-1	2	85	10	5	Coarse sand
9811-31	2	30	60	10	Sandy silt
9811-32	2	25	65	10	Sandy silt
1081-1	14	20	70	10	Sandy silt
1111-1	17	0	50	50	Silty clay
1111-2	17	0	60	40	Clayey silt
1111-4	17	0	20	80	Silty clay
1111-5	17	0	40	60	Silty clay
1111-12	17	0	20	80	Silty clay
1123-1	16	5	20	75	Silty clay
1131-1	10	5	60	35	Clayey silt
1131-2	10	5	45	50	Clayey silt
1141-1	18	5	60	35	Clayey silt
1141-2	18	0	40	60	Silty clay

Component analysis (Numbers in %)

Station-#	Ref.-#	Quartz angular	Quartz rounded	Feldspar	Rock fragments	Mica	Clay	Heavy minerals	Diatoms	Plant debris
9811-1	2	40	20	20	-	-	traces	10	-	traces
9811-31	2	35	15	20	-	-	15	10	traces	5
9811-32	2	30	20	20	-	-	20	15	traces	5
1081-1	14	40	40	10	2	2	3	3	-	-
1111-1	17	30	-	13	-	2	40	15	traces	-
1111-2	17	55	-	-	-	-	35	10	traces	-
1111-4	17	15	7	5	-	-	70	3	-	-
1111-5	17	30	-	4	2	3	50	10	traces	-
1111-12	17	25	-	5	-	-	60	5	5	-
1123-1	16	30	-	5	2	3	50	10	-	-
1131-1	10	40	-	20	-	-	30	9	traces	1
1131-2	10	30	-	15	-	-	50	5	-	-
1141-1	18	30	10	10	-	-	35	15	-	-
1141-2	18	15	5	20	-	-	50	10	traces	-

Table 6: Coarse fraction (>63 µm) content in sea ice sediment samples from the Laptev Sea. Data are presented in Fig. 20.

Station-#	Description	Total sediment (mg)	Coarse fraction > 63µm (mg)	Coarse fraction in % of total sediment
981	47 - 55 cm	575,85	445,40	77,35
9811-2	sea ice	4,781	4,7140	98,60
9811-3	sea ice	1,311	0,1260	9,61
100-1	sea ice	0,215	0,0000	0,00
100-12	0 - 21 cm	84,46	traces	-
1002	sea ice	0,362	0,0000	0,00
1021	30 - 55 cm	0,174	0,0000	0,00
10211	40 - 52 cm	21,53	4,50	20,90
1071	sea ice	0,182	0,0060	3,30
1081-1	sea ice	1,237	traces	-
1081-2	sea ice	0,973	traces	-
108-13	turbid ice	44,73	3,60	8,05
1111-1	sea ice	0,255	0,0080	3,14
1111-3	sea ice	0,371	0,0000	0,00
1111-3b	ice core	159,15	traces	-
1111-4	sea ice	1,858	traces	-
1111-5	sea ice	1,179	traces	-
1111-8	ice core	70,13	0,90	1,28
1111-9	ice core	11,71	0,40	3,42
1122	sea ice	1,358	traces	-
1123	sea ice	0,892	traces	-
1123	0 - 75 cm	0,243	0,0000	0,00
1131-2	sea ice	3,272	1,1890	36,34
1131-3	sea ice	1,317	0,1340	10,17
11312	sea ice	0,914	0,0000	0,00
113-12	0 - 34 cm	110,56	6,20	5,61
11321	sea ice	0,154	0,0000	0,00
1131-5	sea ice	2,649	traces	-
11315	turbid ice	317,93	1,80	0,57
1141-2	sea ice	3,026	0,0580	1,92
11414	turbid ice	831,59	traces	-
114-16	sea ice	256,58	5,40	2,10

Expedition to Novaja Zemlja and Franz Josef Land with RV "Dalnie Zelentsy"

by D. Nürnberg and E. Groth

Dirk Nürnberg, Alfred-Wegener-Institute for Polar and Marine Research (AWI),
Columbusstraße, D-2850 Bremerhaven, F.R.G.
Elke Groth, GEOMAR Research Center for Marine Geosciences, Wischhofstr. 1-3,
D-2300 Kiel 14, F.R.G.

Expedition to Novaja Zemlja and Franz Josef Land with RV "Dalnie Zelentsy"

by D. Nürnberg and E. Groth

Expedition to Novaja Zemlja and Franz Josef Land with RV "Dalnie Zelentsy"

by D. Nürnberg and E. Groth

1. INTRODUCTION

It is generally accepted that the Arctic Ocean is a sensitive area for changes in the global climate. Unfortunately, the short- and long-term geological and climatological development of this area is only unsufficiently known mainly due to major technological and logistical problems when reaching this permanently ice-covered region. First attempts to systematically investigate the geology of the Arctic Ocean area underline the importance of Eurasian shelves as potential source areas for sediments being deposited in the abyssal plains of the Central Arctic Ocean. It has been shown recently that Laptev Sea is a major area where shelf sediments are entrained in Arctic sea ice and subsequently transported through the entire Arctic Ocean via the Transpolar Drift. Whether these large amounts of sea ice sediments contribute to the deep sea sedimentation is disputable. From the comparison of sea ice and deep sea clay mineralogy, oceanic currents and/or gravity flows, tubidity currents etc. across the continental slopes also have to be considered as important steering mechanisms for the sedimentation of terrigeneous material.

The invitation of the "Murmansk Institute of Marine Biology" (Russia) to take part into a ship expedition to the Barents Sea was consequently welcomed to reach areas on the Eurasian shelves, which are very difficult to enter due to logistical and political restrictions. The research vessel "Dalnie Zelentsy", an approximately 40 m long ship not suitable for ice conditions, worked in coastal areas along Novaja Zemlja and Franz Josef Land up to ca. 81 °N. Chief scientist was Dr. G. Tarasov from Murmansk Institute of Marine Biology. For the first time, western scientists were allowed to work along the coast of Novaja Zemlja, which served as a nuclear test area during the sixties and seventies. Franz Josef Land, much more glaciated than Spitsbergen and uninfluenced by the Norwegian-Atlantic Current, has fortunately been reached due to favorable ice conditions. Exactly 120 years ago, this group of islands has been discovered by an Austrian expedition. The archipelago is believed to be a potential source area for kaolinite occurences, which have been found in the Central Arctic Ocean.

In view of a planned joint ship operation of RV "Polarstern" and RV "Dalnie Zelentsy" in 1993 on the Eurasian shelves, this year´s expedition on "Dalnie Zelentsy" was additionally a good opportunity to test the ship´s technical equipment for marine-geological work, especially the possibilities to handle heavy sampling gear provided by the German institutes.

2. BACKGROUND INFORMATION

Generally the Barents shelf is strongly influenced by glacial processes during the last glacial. According to MERKLIN et al. (1992) Quaternary deposits in the southern Barents Sea directly overlie the erosional top of the Upper Cretaceous sedimentary rocks. Glacial moraine deposits are of local distribution on the shelf areas and form extended ranges which mark the extension of glaciers from Novaja Zemlja, Spitsbergen, Franz Josef Land and Scandinavia (MERKLIN et al. 1992; PAVILDIS et al. 1992). Below ca. 200 m (see also PAVILDIS et al. 1992), however, moraine debris is obviously absent being replaced by glaciomarine fine-grained sediments, which have been deposited under ice-covered marine environments. The onset of the Late Weichselian glaciation did not start before 22 ky BP according to ELVERHØI et al. (1992). During the last glacial maximum, the entire Barents Sea was covered by grounded ice being connected with the Fennoscandian Ice Sheet. Ice recession started not before 15 ky BP, and shallowest parts of the northern Barents Sea have not been completely deglaciated before 10 ky BP. Holocene sediments being of varying thicknesses are predominantly fine-grained marine sediments (MERKLIN et al., 1992).

The coastal areas of Novaja Zemlja are characterized by large glacier tongues sliding into the sea. According to LEVCHENKO et al. (1992) the sedimentary deposits in the corresponding bays show distinct differences from south to north. Southern bays are supposed to be estuaries with dark marine clay deposits. In the middle fjords, stratified soft marine and glacial-marine deposits lying in trough-like depressions dominate. Northernmost fjords are characterized by two main depositional types: semiliquid, elastic, light-gray, fine-grained ooze and dark-gray moraine deposits composed of dense sand loam with abundant gravel.

The Franz Josef Land area, consisting of ca. 75 islands at the northeastern edge of the Barents Shelf (total area of about 19,700.km^2), generally shows horizontal sedimentary strata of Upper Triassic to Lower Cretaceous age with a capping of basaltic lavas (HORN 1930). The sedimentary deposits mainly consist of marine clayey shale intercalated with shale, bands of ironstone, and thin layers of lignite. Diabase sills and dykes probably intruded during Lower Cretaceous (DIBNER et al. 1992). The latest geologic history of the archipelago is characterized by postglacial uplift indicated by raised beach terraces, which have been found between sealevel and 30 m (and more!) above this level.

3. RESEARCH OBJECTIVES

Main objective during the RV "Dalnie Zelentsy" Leg 68 from August 15, 1992 to September 5, 1992 was the sampling of shelf bottom sediments including surface samples and long core sections from the coastal areas off Novaja Zemlja and Franz Josef Land as well as from the Barents Shelf. These samples will be added to an already existing sedimentological data base of seafloor sediments at AWI and GEOMAR from the Arctic Ocean being collected during RV "Polarstern" cruises ARK IV/3 and VIII/3, from the Laptev Sea area (E.S.A.R.E. `92 expedition to Kotelnyy Island), and from Fram Strait being sampled during different cruises during the last years. The sedimentological data will be used to reconstruct the paleoceanographic and paleoclimatic evolution of the Arctic areas during the Late Pleistocene and Holocene.

4. COURSE OF EXPEDITION

Starting at Murmansk (Russia) and having visited an Arctic research station of the Murmansk Institute of Marine Biology at Dalnie Zelentsy approximately 180 km east of Murmansk, the ship went straight to Novaja Zemlja where the geological sampling program started at about 73°N and 53°E (Fig. 1). Subsequently, 7 sampling sites (mostly shallower than 150 m) along the coastal

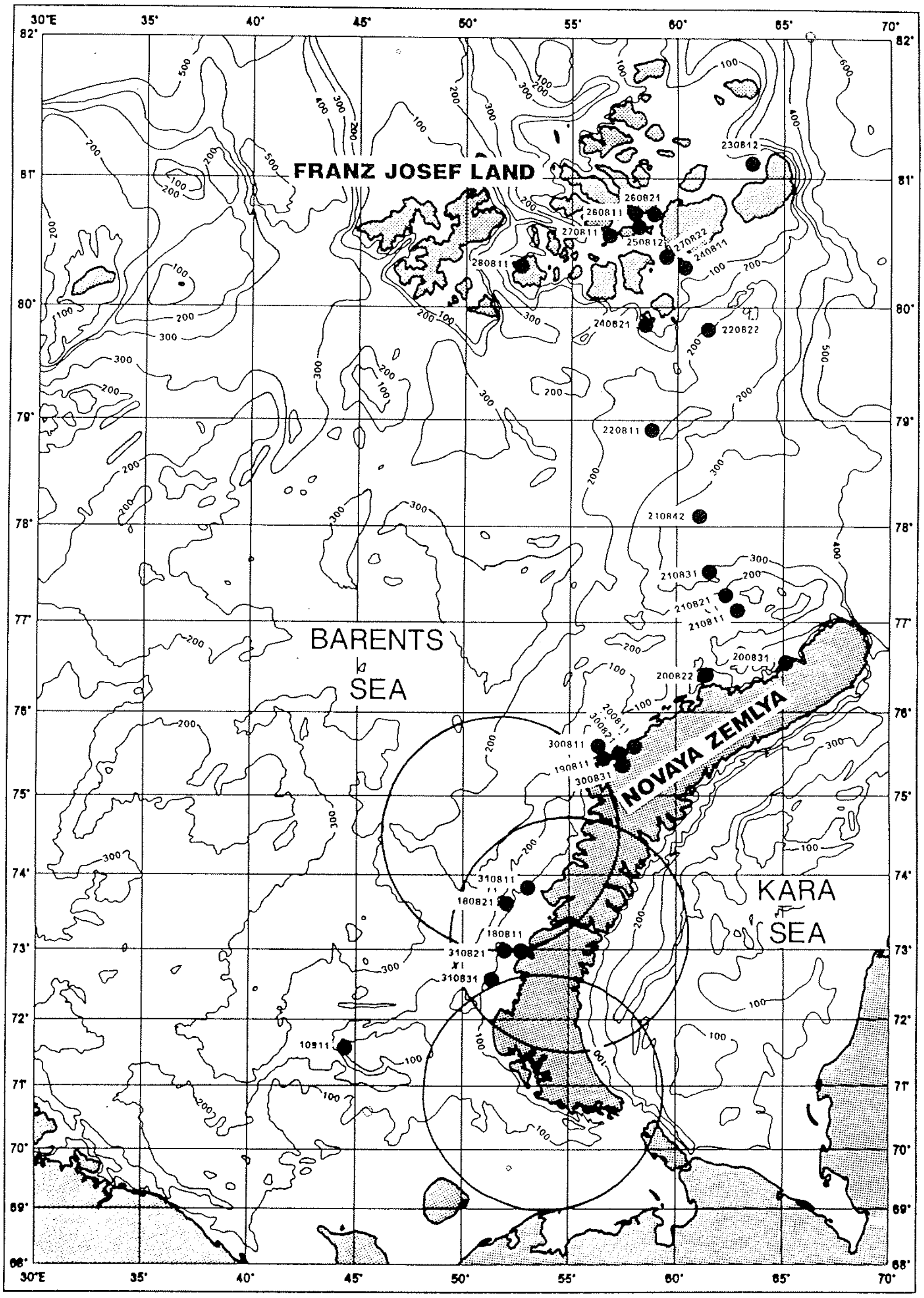

Fig. 1 Bathymetric chart of the eastern Barents Sea including Franz Josef Land and Novaja Zemlja areas. Sampling sites are indicated. Large circles show areas severly influenced by nuclear tests.

areas of Novaja Zemlja have been visited. On the way to Franz Josef Land, a profile of 5 sampling sites has been investigated. Deepest stations reached ca. 415 m. At ca. 78°N and 61°E a prolongation of the ice edge being SE-NW located has been met. The further north we went, the more large icebergs originating from the Franz Josef Land area could be seen. These icebergs were up to 200 m long and up to 40 m high. In the Franz Josef Land archipelago, 9 sites in the vicinity of 8 islands (Wilczek Land, Klagenfurt Island, Greem-Bell Land, Wilczek Island, Hooker Island, Champ Island, Wiener Neustadt Island, Chejsa Island) have been successfully sampled. Water depths here reach from 275 m to 31 m. The ice edge east of Greem-Bell Island has been situated at ca. 81°N and 65°E. Within the archipelago, manoevring was sometimes difficult since sea ice and iceberg drift within the fjords occur rapidly. On the way back, we stopped near by at Admirality Peninsula (Novaja Zemlja) and gained samples from Nordenskiöld Bay in front of a large glacier system. While heading further south, samples have been achieved along the coast of Novaja Zemlja down to 71°35N, 44°24E.

5. METHODS

5.1 Sediment sampling equipment and procedures

For geological, geochemical and biological investigations on seafloor surface samples, box core and van Veen grab were used. For few longer sediment cores the gravity core device onboard RV "Dalnie Zelentsy" was applied (Table 1).

For the first time the box core usually used on German research vessels was operated onboard RV "Dalnie Zelentsy". The device (20 x 28 x 44 cm), which weighs approximately one ton, has been run successfully for 16 times down to water depths of 415 m. Except few attempts, the sediment surface gained by the box core was undisturbed being of considerable importance for the ongoing investigations. However, it has to be mentioned that the operation of such a heavy device is highly problematic and time consuming on a small ship as "Dalnie Zelentsy" is. At high wind speeds with considerable wave action it was impossible. Moreover, the winch system onboard RV "Dalnie Zelentsy" allows only safe operation of the box core down to water depths of approximately 200 m. Below that, strong efforts had to be undertaken to get the device back onboard since the winch system is too weak. For safe operation, at least 6 men including 2 crane operators are necessary. At three sites the core overpenetrated, however, the surfaces could still be used though they were compressed and disturbed. A few times the device did not work due to malfunctions of the trigger mechanism. In average, sediment cores gained by the box corer are 29 cm in length. Maximum core length was 40 cm, minimum is at 12 cm.

Beside the box core, the van Veen grab was applied 10 times to attain approximately 15 cm of seafloor surface sediments. The application of this device was mostly successful though a few malfunctions of the mechanism have been noted. These, however, could still be removed onboard.

Two attempts were made to get longer sediment cores by applying a simple 3 m-gravity corer, which belongs to RV "Dalnie Zelentsy". A removed or highly disturbed surface in addition to severely compression and marginal deformation of core material during sampling procedure, however, causes too many disadvantages for the ongoing analyses.

5.2 Water sampling

Water from 5 m and 50 m depth has been sampled at 17 stations, where geological work has also been performed. Water temperatures have in addition been measured (Table 2). Water samples will be investigated for PCB and oxygen isotopes.

5.3 Sedimentological investigations

The sediment cores gained during the cruise have been routinely photographed, intensively described and graphically displayed. Sediment colors were identified according to the "Munsell Soil Color Charts" (KOLLMORGEN INSTRUMENTS CORP., Newburgh, USA). Samples were coded by "Dalny Zelentsy" DS-numbers and a number code consisting of day, month, number of station and number of device (e.g. 23 08 2 1).

The upper 1 cm of the sediment surface has been systematically sampled for various purposes. The paleontological investigation will include macrobenthos, diatom, foraminifer, and coccolith analyses. Sedimentological work will focus on the grain size, coarse fraction, oxygen isotopes, total organic carbon and clay mineralogy. PCB measurements on surface sediments will be undertaken in conjunction to measurements already performed on Laptev Sea shelf sediments (see DETHLEFF et al. 1993).

The sediment column was sampled every 2 cm for paleontological, geochemical and sedimentological purposes. Syringes injected into the sediment will be used for bulk density measurements, total carbon and carbonate content analyses. Cores taken by the gravity corer have been split into 50 cm long pieces, and subsequently packed into plastic liners, which have not been opened yet.

6. PRELIMINARY RESULTS

6.1 Sedimentology

Along the coast of Novaja Zemlja, 13 shelf bottom samples have been taken. In general, the sediments, which lie in water depths not deeper than 150 m, do not differ significantly from each other. Comparatively coarse sediments, namely silty sand or sandy silts, have been found, which are severly bioturbated by benthic life. Worm tubes (*Polychaets*) have been observed to core depths of ca. 40 cm. Ophiuroideans and bivalves (*Helioptera*, *Cardium*) are common. Dropstones showing a size of more than 10 cm in diameter are abundant at the surface as well as in the entire sediment column. Dark organic rich laminae are visible in all cores down to the core bottoms, however, are mostly destroyed by bioturbation.

A few stations were situated in front of large glacier systems. The belonging sediments are more fine-grained, namely silty clay or clayey silt. A lamination, especially the black organic rich layers, is well evolved since benthic life is rare probably due to high sedimentation rates. According to Tarasov (pers. com.), a cyclic change from the green-gray silty clays or clayey silts to the black laminae can be observed in a few cores.

In the archipelago of Franz Josef Land, samples show a wide variability since they were taken from rather different depths (275 - 31 m). Shallowest stations have uneven sediment surfaces densely covered by ice-rafted detritus. Worm tubes (*Polychaets*) being present through all the sediment column are abundant. Benthic life including barnacles, ophiuroideans, bivalves and worms has drastically evolved. In general, sediments are silty sands or sandy silts showing somewhat lighter colors near the surface than 3-4 cm beyond. Sediments from deeper stations exhibit reduced benthic life and thus, a more intact layering.

6.2 Radioactive pollution

Novaja Zemlja has been test area for nuclear explosions for a long time. The chart "Barents Sea - Biological resources and human impact" prepared by MATISHOV (1991) outlines areas of atmospheric, marine or underground nuclear explosions on Novaja Zemlja. In 1990, GREENPEACE measured up to 40 µSv/h in an underground pit 3 km inland Novaja Zemlja, which is a quite high dose. According to SZCZYPA et al. (1992) radionuclides produced by nuclear explosions can rapidly be accumulated by plankton and algae. Since these organisms serve as food for higher trophic levels, radionuclides become concentrated in organisms such as oysters, clams, shrimp etc. The probability for incorporation of radionuclides into recent sedimentary deposits consequently was suspected.

Since the cruise was supposed to focus on this nuclear test area, a dose rate meter for Gamma radiation has been applied. Measurements have been undertaken on land, next to shelf bottom sediments and continuously in the atmosphere during the entire cruise (Table 1), especially in areas of atomic bomb tests indicated in the map of MATISHOV (1991).

The average value being measured is 0.071 µSv/h. Next to shallow marine sediments, maximum radiation is about 0.106 µSv/h and lowest radiation is about 0.028 µSv/h. The highest value of 0.179 µSv/h has been measured on Novaja Zemlja (Bezymannaya Bay) in the vicinity of the GREENPEACE working area. However, all measurements can be accounted for natural radiation, which is in the range of approximately 50 to 200 nSv/h (equals 0.05 to 0.20 µSv/h). Our results are concordant with SZCZYPA et al. (1992), who could not detect unnatural high levels of radioactive radiation.

7. ACKNOWLEDGEMENTS

We would like to thank Prof. Dr. G. Matishov, Director of "Murmansk Institute of Marine Biology" (Russia) for inviting us to take part in the expedition to the Russian Arctic. Also, we thank Dr. G. Tarasov, chief-scientist onboard RV "Dalnie Zelentsy", who helped to solve all logistical problems. Without the crew of RV "Dalnie Zelentsy" and members of the "Murmansk Institute of Marine Biology" we would not have been able to gather this data set. For discussion we gratefully thank Dr. H. Kassens. Thanks are also due to Prof. Dr. D. Fütterer, Dr. Stein (AWI), and Prof. Dr. J. Thiede (GEOMAR), who encouraged this work.

8. REFERENCES

Dethleff, D., Nürnberg, D., Reimnitz, E., Saarso, M. & Savchenko, Y.P. (1993): East Siberian Arctic Region Expedition '92: The Laptev Sea - Its significance for Arctic sea-ice formation and Transpolar sediment flux. - Ber. Polarforsch. (this volume).

Dibner, V., Bro, E., Pchelina, T., Preobrarajenskaja, E, Shkola, I., Embry, E. & Mørk, A. (1992): Geology of the Franz Josef Land archipelago, Russian Republic. - Int. Conf. Arct. Marg. (ICAM 1992), Anchorage, Alaska, USA.

Elverhøi, A., Solheim, A., Nyland-Berg, M. & Russwurm, L. (1992): Last interglacial-glacial cycle, Western Barents Sea. - LUNDQUA Report, 35, 17-24.

Horn, G. (1930): Franz Josef Land - Natural history, discovery, exploration, and hunting. -Srifter om Svalbard og Ishavet, 29, 54 pp.

Levchenko, O.V., Dunaev, N.N., Merklin, L.R. & Pavlidis, Yu.A. (1992): The sediment cover structure of the western Novaya Zemlya Bays. - Int. Conf. Arct. Marg. (ICAM 1992), Anchorage, Alaska, USA.

Matishov, G. (1991) Problems of the Arctic nature protection. - Polar Session, Arctic Environment Research, Wyprawy Geograficzne na Spitsbergen, UMCS, Lublin.

Merklin, L.R., Dunaev, N.N., Levchenko, O.V. & Pavlidis, Yu.A. (1992): The Quaternary deposits of the Barents Sea. - Int. Conf. Arct. Marg. (ICAM 1992), Anchorage, Alaska, USA.

Pavildis, Yu.A., Dunaev, N.N., Levchenko, O.V. & Merklin, L.R. (1992): The Late Pleistocene paleogeography of the Eurasia Arctic shelf. - Int. Conf. Arct. Marg. (ICAM 1992), Anchorage, Alaska, USA.

Szczypa, J., Janusz, W, Solecki, J., Matishov, G.G. & Matishov, D.G. (1992): The investigation of concentration of radionuclides in the sediments in the Barents Sea. - Wyprawy Geograficzne na Spitsbergen, UMCS, Lublin, 179-189.

9. APPENDIX

Table 1 Geographical locations and technical data of sediment cores and sediment surface samples gained during the cruise. Gamma radiation measured on sediment surfaces is indicated.

Sediment samples									
Station-#	DS-#	Locality	Latitude (°N)	Longitude (°E)	Water depth (m)	Radiation Sediment (µSv/h)	Sample type	Gain (cm)	Remarks
180811	68-1	Novaja Semlya	72°59,08	053°03,38	28	0.080-0.100	Box core	12,00	0.048-0.178 µSv/h on land
180821	68-2	off Novaja S.	73°35,98	052°16,48	137	no data	Box core	23,00	
180822	68-2	off Novaja S.	73°35,98	052°16,48	137	no data	Dredge		
190811	68-3	off Novaja S.	75°28,23	056°46,06	138	0.057-0.061	Box core	31,50	
200811	68-4	Velkitsky Bay	75°35.50	057°59,00	53	0.057	Box core	31,50	
200822	68-5	off Novaja S.	76°25,39	061°23,72	53	no data	Box core	ca. 20	
200831	68-6	Russian Bay	76°28,50	065°11,80	150	0.050	van Veen grab	ca. 15	
200833	68-6	Russian Bay	76°28,50	065°11,80	150	0.050	Gravity core	91,00	
210811	68-7	off Novaja S.	77°08,60	062°50,30	100	0.028-0.071	van Veen grab	ca. 15	
210821	68-8	off Novaja S.	77°19,40	062°16,90	219	0.078	Box core	29,00	
210831	68-9	off Novaja S.	77°33,20	061°30,70	320	no data	van Veen grab	ca. 15	
210833	68-9	off Novaja S.	77°33,20	061°30,70	320	no data	Gravity core	70,00	Not opened yet
210842	68-10	off Novaja S.	78°03,66	061°11,20	415	0.087	Box core	36,00	
220811	68-11	off Novaja S.	78°54,50	059°00,00	260	0.078	Box core	40,00	
220822	68-12	off FJL	79°50,00	061°29,00	145	0.093-0.064	Box core	21,00	
230812	68-13	Greem Bell Island	81°07,11	063°31,57	275	no data	van Veen grab	ca. 15	First sight of ice edge
240811	68-15	Klagenfurt	80°20,57	060°19,94	37	0.079	van Veen grab	ca. 15	
240821	68-16	Wilczek Island	79°52,87	058°40,97	43	0.079-0.045	Box core	21,00	
250812	68-17	Chejsa Island	80°37,20	058°05,80	34	0.076	van Veen grab	ca. 15	
260811	68-19	Wiener Neustadt	80°44,30	057°53,80	29	0.058	van Veen grab	ca. 15	No gain
260821	68-20	Wiener Neustadt	80°43,90	058°52,90	160	0.087-0.057	Box core	40,00	
270811	68-23	Camp	80°30,40	056°43,80	214	0.103-0.058	Box core	32,00	
270822	68-24	Wilczek Land	80°24,04	059°37,75	31	0.106-0.081	van Veen grab	ca. 15	
280811	68-25	Hooker Island	80°19,92	052°50,00	49	0.073-0.051	Box core	ca. 1	Over-penetrated
300811	68-31	Nordenskiöld Bay	75°33,3	056°26,70	165	0.060	Box core	31	
300821	68-32	Nordenskiöld Bay	75°28,50	057°10,00	120	0.058-0.068	Box core	28	
300831	68-33	Nordenskiöld Bay	75°21,50	057°35,80	45	0.066-0.060	Box core	31	
310811	68-35	off Novaja S.	73°50,00	053°00,00	120	0.077	van Veen grab	ca. 15	
310821	68-37	off Novaja S.	73°00,63	051°53,64	70		van Veen grab	ca. 15	
310831	68-38	off Novaja S.	72°36,90	051°21,90	85	0.081	van Veen grab	ca. 15	
10911	68-39	off Novaja S.	71°35,10	044°24,70	85	0.052	Box core	9,00	

Table 2 Geographical locations of water sampling sites. Water temperatures are indicated.

Water samples

Station-#	DS-#	Locality	Latitude (°N)	Longitude (°E)	Water depth (m)	Sample type	Water samples Depth (m)	Water temp. (°C)
190821	68-3	Velkitsky Bay	75°28,03	056°44,17	139	Water bottle	5,00	?
						Water bottle	10,00	?
						Water bottle	20,00	2,50
						Water bottle	50,00	1,00
200821	68-5	off Novaja S.	76°25,39	061°23,72	53	Water bottle	5,00	3,50
						Water bottle	40,00	-
200832	68-6	Russian Bay	76°28,50	065°11,80	150	Water bottle	5,00	2,00
						Water bottle	50,00	1,00
210822	68-8	off Novaja S.	77°19,40	062°16,90	219	Water bottle	5,00	0,50
						Water bottle	50,00	1,20
210824	68-8	off Novaja S.	77°29,40	061°42,32	335	Water bottle	5,00	2,00
210841	68-10	off Novaja S.	78°03,66	061°11,20	415	Water bottle	5,00	3,00
						Water bottle	50,00	-1,00
220812	68-11	off Novaja S.	78°54,50	059°00,00	260	Water bottle	5,00	3,00
						Water bottle	50,00	1,00
220821	68-12	off FJL	79°50,00	061°29,00	145	Water bottle	5,00	1,25
						Water bottle	50,00	-1,00
230811	68-13	Greem Bell Island	81°07,11	063°31,57	275	Water bottle	5,00	-1,50
						Water bottle	50,00	-1,25
240822	68-16	Wilczek Island	79°52,87	058°40,97	43	Water bottle	5,00	-0,50
250811	68-17	Chejsa Island	80°37,20	058°05,80	34	Water bottle	5,00	1,00
						Water bottle	34,00	-1,00
260812	68-19	Wiener Neustadt	80°44,30	057°53,80	29	Water bottle	5,00	-1,50
270821	68-24	Camp	80°24,04	059°37,75	40	Water bottle	5,00	-1,00
						Water bottle	40,00	-1,20
280812	68-25	Hooker Island	80°19,92	052°50,00	49	Water bottle	5,00	-1,00
						Water bottle	45,00	-1,00
300812	68-31	Nordenskiöld Bay	75°33,30	056°26,70	165	Water bottle	5,00	4,00
						Water bottle	50,00	3,25
310822	68-37	off Novaja S.	73°00,63	051°53,64	70	Water bottle	5,00	6,00
						Water bottle	50,00	4,25
310832	68-38	off Novaja S.	72°36,90	051°21,90	85	Water bottle	5,00	5,75
						Water bottle	50,00	6,00
10912	68-39	off Novaja S.	71°35,10	044°24,70	85	Water bottle	5,00	7,00
						Water bottle	50,00	-

Legend

- Sand
- Sandy silt
- Sandy silty clay
- Silty clay
- Bioturbation
- Laminae / single thin layers
- Drop stones
- Uneven sharp contact
- Horizontal sharp contact
- Coarsening upwards sequence
- Fining upwards sequence

Rock colors

according to "Munsell Soil Color Charts" (Kollmorgen Instruments Corp., Newburgh, USA, 1990)

HUE 2.5Y	2.5Y2/0	Black
	2.5Y3/2	Very dark grayish brown
	2.5Y3/3	Dark olive brown
	2.5Y4/2	Dark grayish brown
	2.5Y4/3	Olive brown
HUE 5Y	5Y2.5/1	Black
	5Y2.5/2	Black
	5Y3/1	Very dark olive gray
	5Y3/2	Dark olive gray
	5Y4/1	Dark gray
	5Y4/2	Olive gray
	5Y4/3	Olive
	5Y5/1	Gray
HUE 10YR	10YR2/2	Very dark brown
	10YR3/3	Dark brown
HUE 7.5YR	7.5YR3/2	Dark brown

GKG Description	Core Number	Gear: Box core
		Length: 12 cm
	180811 - DS 68-1	Water depth: 28 m
		72°59.08 N 053°03.38 E

Lithology	Color Texture	Description, Remarks, etc.	Investigator: Nürnberg/Groth	Date: Aug. 18, 92
Surface	5Y2.5/2 5Y2.5/1 5Y3/1	fine to coarse sand with gravel up to 1 cm in diameter, only minor clay and silt portions, calcareous foraminifers, worm tubes (polychaets), ophiuroideans (reddish, -3 cm in diameter) common, in uppermost cm white clams (-1 cm in diameter), varying colors		
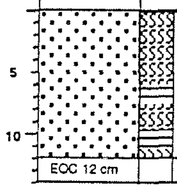	5Y2.5/2 5Y2.5/1 5Y3/1	fine to coarse sand with gravel up to 1 cm in diameter, only minor clay and silt portions, bioturbation through all the sediment column, worm tubes (polychaets, -1 cm in diameter and -5 cm in length) abundant down to core bottom, pelecypods common in 5-8 cm depth, black organic rich laminated areas all over profile		

GKG Description	Core Number	Gear: Box core
		Length: 23 cm
	180821 - DS 68-2	Water depth: 137 m
		73°35.98 N 052°15.48 E

Lithology	Color Texture	Description, Remarks, etc.	Investigator: Nürnberg/Groth	Date: Aug. 18, 92
Surface	5Y3/2	sandy silt to silty sand, densely covered by dropstones (-30 cm in diameter, rounded and angular), pelecypod fragments (-3 cm) and worm tubes (polychaets) common, barnacles (-8 cm in length) dredge from same station shows rich benthic life: crabs, pelecypods, fish, sponges, ophiuroideans		
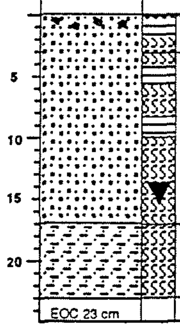	5Y3/2	sandy silt to silty sand, coarse material, dropstones		
		sandy silt to silty sand, becoming more fine-grained with depth, areas of black organic rich laminae between 10 cm and 17 cm: oxidized reddish spots		
		silty clay, very stiff		

GKG Description	Core Number	Gear: Box core
	190811 - DS 68-3	Length: 31.5 cm
		Water depth: 138 m
		75°28.23 N 056°46.06 E

Lithology	Color Texture	Description, Remarks, etc.	Investigator: Nürnberg/Groth	Date: Aug. 19, 92
Surface	5Y3/1-3/2	clayey silt densely covered by dropstones (-2 cm in diameter, uneven surface, rich in worm tubes (polychaets) and pelecypods (-3 cm in length)		
	5Y3/1-3/2	clayey silt to silty clay, bioturbation down to core bottom, black organic rich laminae		
	5Y3/1-3/2	at 23 cm - 31 cm: large angular dropstone		
EOC 31.5 cm				

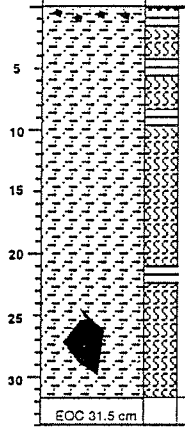

GKG Description	Core Number	Gear: Box core
	200811 - DS 68-4	Length: 31.5 cm
		Water depth: 53 m
		75°35.50 N 057°59.00 E

Lithology	Color Texture	Description, Remarks, etc.	Investigator: Nürnberg/Groth	Date: Aug. 20, 92
Surface	5Y4/3	silty clay, uneven surface, only few ophiuroideans (glacier suspension)		
	5Y4/3	silty clay, brownish oxydized speckles down to 20 cm core depth, black organic rich laminae all over the profile core taken in front of a large glacier on Novaja Zemlja		
EOC 31.5 cm				

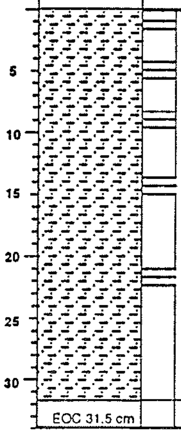

GKG Description	Core Number	Gear:	Box core
		Length:	20 cm
	200822 - DS 68-5	Water depth:	53 m
		76°25,39 N	061°23,72 E

Lithology	Color Texture	Description, Remarks, etc.	Investigator: Nürnberg/Groth	Date: Aug. 20, 92
Surface	5Y4/1	coarse sand with minor clay and silt portions, large dropstones (-3 cm in diameter) common, rich in biogenic fragments (clams), few ophiuroideans core is severely damaged since the box core hit a large stone at the seafloor		
0–20 cm	5Y4/1	coarse sand with minor clay and silt portions, large dropstones (-3 cm in diameter) common, rich in biogenic fragments (clams), few ophiuroideans		
EOC 20 cm				

BG Description	Core Number	Gear:	van Veen grab
		Length:	ca. 15 cm
	200831 - DS 68-6	Water depth:	150 m
		76°28,50 N	065°11,80 E

Lithology	Color Texture	Description, Remarks, etc.	Investigator: Nürnberg/Groth	Date: Aug. 20, 92
Surface	5Y5/1 2.5Y2/0	silty clay, worm tubes (polychaets) and small pelecypods (up to 1 cm in diameter) common, surface is damaged		
0–15 cm	5Y5/1 2.5Y2/0	silty clay, worm tubes (polychaets) and small pelecypods (up to 1 cm in diameter) common, surface is damaged		
EOC ca. 15 cm				

Core Description

Core Number	Gear: Gravity core
200833 - DS 68/6	Length: 91 cm
	Water depth: 150 m
	76°28,50 N 065°11.80 E

Investigator	Date
Nürnberg/Groth	Aug. 20, 92

Lithology	Color Texture	Description, Remarks, etc.
0–70	5Y5/1	clayey silt, homogeneous black organic rich laminae all over the profile, especially at 30-31 cm, 57-59 cm, 70-74 cm, 84-86 cm dropstones (-2 cm in diameter) abundant at 40–42 cm
70–91	5Y5/1	clayey silt, becoming increasingly sandy at core bottom

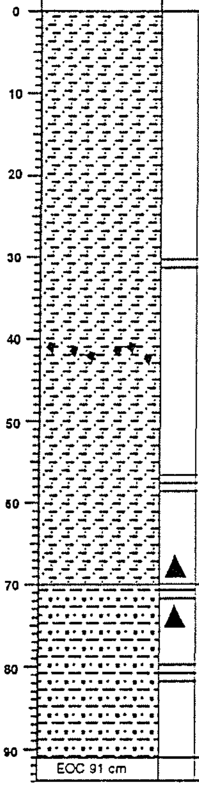

BG Description

Core Number	Gear: van Veen grab
210811 - DS 68-7	Length: ca. 15 cm
	Water depth: 100 m
	77°08,60 N 062°50,0 E

Investigator	Date
Nürnberg/Groth	Aug. 21, 92

Lithology	Color Texture	Description, Remarks, etc.
Surface	5Y3/2	silty fine sand disturbed surface densely covered by dropstones (-3 cm in diameter), ophiuroideans (-3 cm) common, 1 echinoderm (5 cm), worm tubes (polychaets) all over the profile
0–15	5Y3/2	silty fine sand worm tubes (polycheats) all over the profile, few dropstones all over sediment column

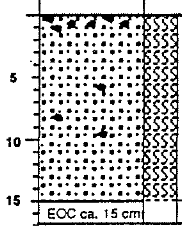

GKG Description	Core Number	Gear:	Box core
		Length:	29 cm
	210821 - DS 68-8	Water depth:	219 m
		77°19,40 N	062°16,90 E

Lithology	Color Texture	Description, Remarks, etc.	Investigator: Nürnberg/Groth	Date: Aug. 21, 92
Surface	5Y3/1 - 5Y3/2	clayey silt, surface densely covered by rounded and angular dropstones (0.5 - 2 cm in diameter), uneven surface, pelecypod fragments (Helioptera, 1.5 - 2 cm in length), ophiuroideans and polychaets common		
	5Y3/1 - 5Y3/2	clayey silt, pelecypod fragments (Helioptera, 1.5 - 2 cm in length), ophiuroideans and polychaets common		
	5Y3/1 - 5Y3/2	sandy silt to silty sand, very stiff sediment black organic rich laminae all over the sediment column, mainly concentrated between 12 cm and 14 cm concentration of dropstones at 15-18 cm in general, dropstones and worm tubes (polychaets) appear all over the profile bioturbation down to core bottom, indicated by reddish, oxygenized colors		
EOC 29 cm				

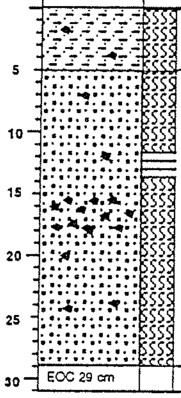

BG Description	Core Number	Gear:	van Veen grab
		Length:	ca. 15 cm
	210831 - DS 68-9	Water depth:	320 m
		77°33,20 N	061°30,70 E

Lithology	Color Texture	Description, Remarks, etc.	Investigator: Nürnberg/Groth	Date: Aug. 21, 92
Surface	5Y4/3	silty fine sand uneven surface, only few ophiuroideans		
	5Y4/3	silty fine sand uneven surface, only few ophiuroideans		
EOC ca. 15 cm				

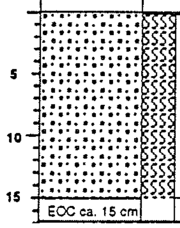

GKG Description	Core Number	Gear: Box core
		Length: 36 cm
	210842 - DS 68-10	Water depth: 415 m
		78°03.66 N 061°11.20 E

Investigator	Date
Nürnberg/Groth	Aug. 21, 92

Lithology	Color Texture	Description, Remarks, etc.
Surface	10YR3/3	silty clay, light brown colors with black patches sediment surface is highly disturbed and compressed since core overpenetrated, however, surface is not missing
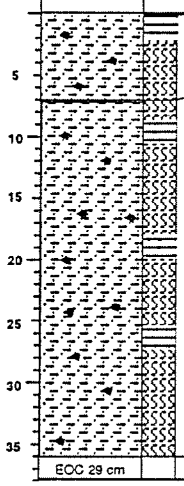	10YR3/3	silty clay, light brown colors with black patches
	5Y4/2	brownish surface sediments grade into gray silty clay, homogeneous, black organic rich laminae all over the profile, worm tubes (polychaets) and dropstones down to core bottom bioturbation down to core bottom, indicated by reddish, oxygenized colors
EOC 29 cm		

GKG Description	Core Number	Gear:	Box core
	220811 - DS 68-11	Length:	40 cm
		Water depth:	260 m
		78°54,50 N 059°00,00 E	

Lithology	Color Texture	Description, Remarks, etc.	Investigator	Date
			Nürnberg/Groth	Aug. 22, 92
Surface	10YR3/3	clayey silt, light brown colors with black patches sediment surface is highly disturbed and compressed since core overpenetrated, however, surface is not missing		

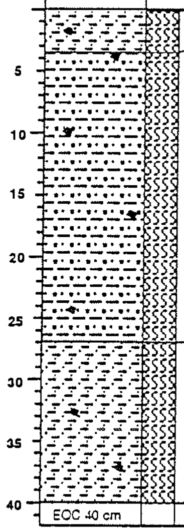

Color Texture	Description, Remarks, etc.
10YR3/3	clayey silt, light brown colors with black patches (manganese and iron oxides (7.5YR3/2))
5Y3/2	sandy clayey silt light brownish oxidized layers intercalated at 4-5 cm, 5.5-7 cm, and 12-13 cm, uneven boundaries bioturbation down to core bottom, indicated by reddish, oxygenized colors, especially between 7-27 cm
5Y3/2	clayey silt black organic rich laminae are intercalated, worm tubes (polychaets) occur all over the sediment column

EOC 40 cm

GKG Description	Core Number	Gear:	Box core
	220822 - DS 68-12	Length:	21 cm
		Water depth:	145 m
		79°50,00 N 061°29,00 E	

Lithology	Color Texture	Description, Remarks, etc.	Investigator	Date
			Nürnberg/Groth	Aug. 22, 92
Surface	2.5Y42 - 2.5Y4/3	sandy silt to silty sand, uneven surface, slightly disturbed by coring, small dropstones (-0.5 cm in diameter), ophiuroideans (-5 cm in diameter), and hydrozoans common, worm tubes (polychaets)		

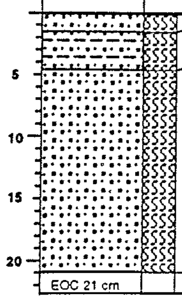

Color Texture	Description, Remarks, etc.
2.5Y4/2-4/3	sandy silt to silty sand
10YR2/2	clayey sandy silt, very stiff, falls into small plates
5Y3/1	sandy silt, homogeneous, sometimes spotty (10YR2/2)

EOC 21 cm

BG Description	Core Number		
	230812 - DS 68-13	Gear:	van Veen grab
		Length:	ca. 15 cm
		Water depth:	275 m
		81°07.11 N 063°31.57 E	
		Investigator	Date
		Nürnberg/Groth	Aug. 23, 92

Lithology	Color Texture	Description, Remarks, etc.
Surface	10YR3/3	sandy silt, uneven surface, 1 shell fragment
	10YR3/3	sandy silt,
	5Y3/2	silty clay to clayey silt, homogeneous, gray color

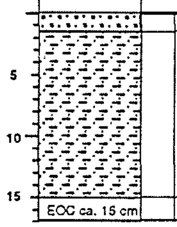

BG Description	Core Number		
	240811 - DS 68-15	Gear:	van Veen grab
		Length:	ca. 15 cm
		Water depth:	37 m
		80°20.57 N 060°19.94 E	
		Investigator	Date
		Nürnberg/Groth	Aug. 24, 92

Lithology	Color Texture	Description, Remarks, etc.
Surface	2.5Y3/3	silty sand, uneven surface, densely covered by pelecypod fragments, dropstones (-10 cm in diameter), and ophiuroideans (-3 cm in diameter), rich in calcareous foraminifers and polychaets
	2.5Y3/3	silty sand, uneven surface, densely covered by pelecypod fragments, dropstones (-10 cm in diameter), and ophiuroideans (-3 cm in diameter), rich in calcareous foraminifers and polychaets, dropstones all over sediment column

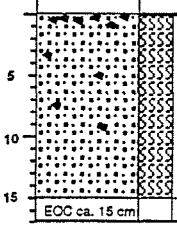

GKG Description	Core Number	Gear:	Box core
		Length:	21 cm
	240821 - DS 68-16	Water depth:	43 m
		79°52.87 N	058°40.97 E
		Investigator	Date
		Nürnberg/Groth	Aug. 24, 92

Lithology	Color Texture	Description, Remarks, etc.
Surface	5Y4/2	silty sand, uneven surface, densely covered by dropstones (0.5 cm - 2 cm in diameter), pelecypods (Helioptera) and pelecypod fragments (-3 cm in length) abundant, ophiuroideans, hydrozoans and anthozoans (10 cm in length) are common
	5Y4/2	silty sand, 1 dropstone (5 cm in diameter) with hydrozoans, few oxidized spots
	5Y4/2	silty sand, very stiff, somewhat finer than at surface, with black organic rich speckles all over the sediment column, dropstones and shell fragments abundant down to core bottom
EOC 21 cm		

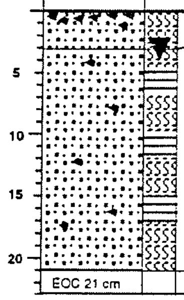

BG Description	Core Number	Gear:	van Veen grab
		Length:	ca. 15 cm
	250812 - DS 68-17	Water depth:	36 m
		80°37.20 N	058°05.80 E
		Investigator	Date
		Nürnberg/Groth	Aug. 25, 92

Lithology	Color Texture	Description, Remarks, etc.
Surface	5Y3/2	silty sand to sandy silt, densely covered by benthos and dropstones (- 8 cm in diameter): barnacles settling on bivalve shells, Helioptera shells, echinoderms, ophiuroideans, polychaets, algae, holothuroideans, Mya truncata, large bryozoan colonies
	5Y3/2	silty sand to sandy silt, uneven surface, dropstones and worm tubes (polychaets) down to core bottom
EOC ca. 15 cm		

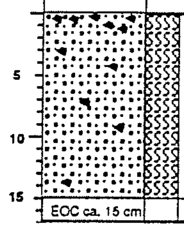

GKG Description	Core Number	Gear: Box core
		Length: 40 cm
	260821 - DS 68-20	Water depth: 160 m
		80°43,90 N 058°52,90 E

Investigator	Date
Nürnberg/Groth	Aug. 28, 92

Lithology	Color Texture	Description, Remarks, etc.
Surface	5Y3/2	clayey silty sand, uneven surface, few worm tubes (polychaets) sticking out of the sediment surface
	5Y3/2	clayey silty sand, uneven surface, few worm tubes (polychaets)
	5Y2.5/1	sandy silt, slightly darker than surface layer black organic rich laminae all over the sediment column, especially concentrated at 7-15 cm, 35-40 cm oxidized burrows with material from surface between 22-27 cm, 34-38 cm dropstone (4 cm in diameter) at 17-19 cm

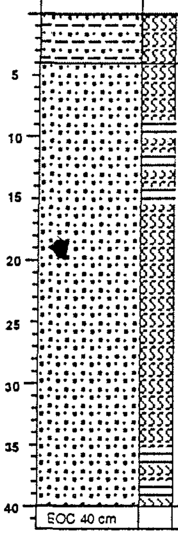

GKG Description	Core Number	Gear: Box core
		Length: 32 cm
	270811 - DS 68-23	Water depth: 214 m
		80°30,40 N 056°43,80 E

Investigator	Date
Nürnberg/Groth	Aug. 27, 92

Lithology	Color Texture	Description, Remarks, etc.
Surface	5Y3/2	silty sand to sandy silt, uneven surface, slightly disturbed by coring, densely settled by polychaets, rich in dropstones (< 0.5 cm in diameter)
	5Y3/2	silty sand to sandy silt, densely settled by polychaets, rich in dropstones (< 0.5 cm in diameter)
	5Y3/1	sandy silt, slightly darker than surface layer, oxidized light brownish patches and spots all over the sediment column due to bioturbation
EOC 32 cm		

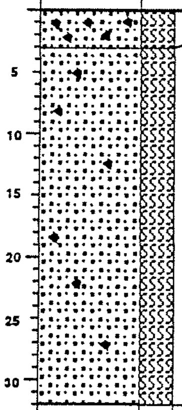

BG Description	Core Number	Gear: van Veen grab
		Length: ca. 15 cm
	270822 - DS 68-24	Water depth: 31 m
		80°24,04 N 059°37,75 E

Investigator	Date
Nürnberg/Groth	Aug. 27, 92

Lithology	Color Texture	Description, Remarks, etc.
Surface	5Y3/1	silty sand, rich in benthic life: large bryozoan colonies covering all surface, Mya truncata and Helioptera shells, worm tubes (polychaets), barnacles
		silty sand
	2.5Y3/2	silty sand, slightly darker than above
EOC ca. 15 cm		

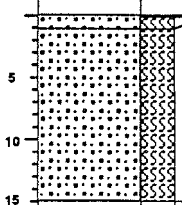

GKG Description	Core Number	Gear: Box core
	280811 - DS 68-25	Length: 1 cm
		Water depth: 49 m
		80°19,92 N 052°50,00 E

Lithology	Color Texture	Description, Remarks, etc.	Investigator: Nürnberg/Groth	Date: Aug. 28, 92
Surface	5Y3/2	silty sand , uneven surface (glacier suspension), severely disturbed by coring, core overpenetrated and compressed, sediment is very soft, few oxidized worm tubes (polychaets)		
	5Y3/2	silty sand		
EOC 1 cm				

GKG Description	Core Number	Gear: Box core
	300811 - DS 68-31	Length: 31 cm
		Water depth: 165 m
		75°33,30 N 056°26,70 E

Lithology	Color Texture	Description, Remarks, etc.	Investigator: Nürnberg/Groth	Date: Aug. 30, 92
Surface	5Y3/2	silty sand , uneven surface, dropstones (- 1cm in diameter) and worm tubes (polychaets) common, living bivalves in the upper 3 cm of sediment (Cardium sp.), ophiurideans (-3 cm in diameter) common, 1 snail house (Turitella ???)		
	5Y3/2	silty sand, see surface		
5 – 10 – 15 – 20	5Y2.5/1	silty sandy clay, black organic rich laminae are intercalated, severely bioturbated		
25 – 30	5Y2.5/1	sandy silty clay, few black laminae, more homogeneous than above		
EOC 31 cm				

GKG Description	Core Number	Gear: Box core
	300821 - DS 68-32	Length: 28 cm
		Water depth: 120 m
		75°28,50 N 057°10,00 E

Lithology	Color Texture	Description, Remarks, etc.	Investigator: Nürnberg/Groth	Date: Aug. 30, 92
Surface	5Y4/1	clayey silt with minor sand portion, uneven surface, few dropstones and few worm tubes (polychaets), only 1 bivalve fragment		
	5Y4/1	clayey silt with minor sand portion, uneven surface, see surface, pelecypods in upper 3 cm		
	5Y3/1	clayey silt with minor sand portion, uneven surface, black organic rich laminae and patches all over sediment column, surface material mixed down to core bottom due to bioturbation		

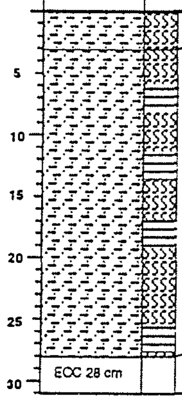

GKG Description	Core Number	Gear: Box core
	300831 - DS 68-33	Length: 31 cm
		Water depth: 45 m
		75°21.50 N 057°35.80 E

Lithology	Color Texture	Description, Remarks, etc.	Investigator: Nürnberg/Groth	Date: Aug. 30, 92
Surface	5Y4/1	silty clay, uneven surface, bivalve shells in the upper top centimeters, only small dropstones (<0.5 mm), very soft sediment		

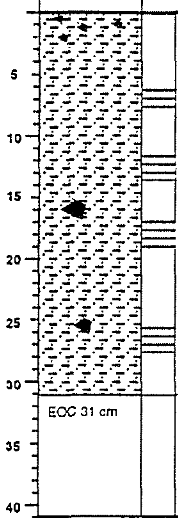

Color Texture	Description, Remarks, etc.
5Y4/1	silty clay, black organic rich laminae and patches all over the sediment column, very soft sediment, bioturbation not evident, few droptones and bivalve shells (glacier suspension)
5Y3/1	at 15-17 cm dropstone
	at 25-27 cm dropstone

EOC 31 cm

in sediment core taken by Tarasov, cyclic deposition of silty clay and black organic rich layers can be observed, layers become thinner the deeper in the sediment column they are
hypothesis: annual variations in sedimentation (winter and summer deposits)

BG Description	Core Number	Gear: van Veen grab
	310811 - DS 68-35	Length: ca. 15 cm
		Water depth: 120 m
		73°50.00 N 053°00.00 E

Lithology	Color Texture	Description, Remarks, etc.	Investigator: Nürnberg/Groth	Date: Aug. 31, 92
Surface	5Y3/1	silty sand, densely packed with different kinds of dropstones (-10 cm in diameter), worm tubes (polychaeta), Helioptera, Cardium sp., Sipunculida		

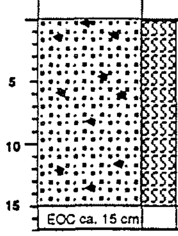

Color Texture	Description, Remarks, etc.
5Y3/1	silty sand, densely packed with different kinds of dropstones (-10 cm in diameter), worm tubes (polychaeta), Helioptera, Cardium sp., Sipunculida

EOC ca. 15 cm

BG Description	Core Number	Gear: van Veen grab
	310821 - DS 68-37	Length: ca. 15 cm
		Water depth: 70 m
		73°00.63 N 051°53.64 E

Lithology	Color Texture	Description, Remarks, etc.	Investigator	Date
			Nürnberg/Groth	Aug. 31, 92
Surface	5Y4/1	silty sand, densely packed with different kinds of dropstones (-10 cm in diameter), worm tubes (polychaets), Helioptera, Cardium sp., Sipunculida, ophiuroideans, abundant in echinoderms, barnacles settling on dropstones, snails		
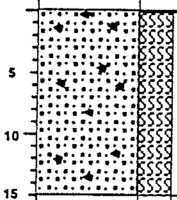	5Y4/1	silty sand, densely packed with different kinds of dropstones (-10 cm in diameter), worm tubes (polychaets), Helioptera, Cardium sp., Sipunculida, ophiuroideans, abundant in echinoderms, barnacles settling on dropstones, snails		
EOC ca. 15 cm				

BG Description	Core Number	Gear: van Veen grab
	310831 - DS 68-38	Length: ca. 15 cm
		Water depth: 85 m
		72°36,90 N 051°21,90 E

Lithology	Color Texture	Description, Remarks, etc.	Investigator	Date
			Nürnberg/Groth	Aug. 31, 92
Surface	5Y4/3	silty sand, densely packed with different kinds of dropstones (-20 cm in diameter), barnacles, crabs, ophiuroideans, echinoderms, bivalve shells, Helioptera common		
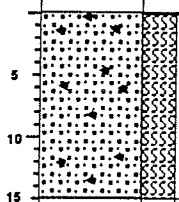	5Y4/3	silty sand, densely packed with different kinds of dropstones (-20 cm in diameter), barnacles, crabs, ophiuroideans, echinoderms, bivalve shells, Helioptera common		
EOC ca. 15 cm				

GKG Description	Core Number	Gear: Box core
		Length: 9 cm
	010911 - DS 68-39	Water depth: 85 m
		71°35.10 N 044°24.70 E

Investigator	Date
Nürnberg/Groth	Sept.1, 92

Lithology	Color Texture	Description, Remarks, etc.
Surface	2.5Y4/2	coarse sand, worm tubes (polychaets) sticking out of the sediment surface by 5 cm, bivalve shells (Clamys, Helioptera), barnacles, worms abundant, dropstones (-1 cm in diameter) abundant
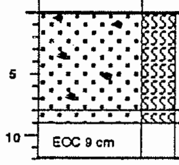	2.5Y4/2	coarse sand, worm tubes (polychaets), bivalve shells (Clamys, Helioptera), barnacles, worms abundant, dropstones (-1 cm in diameter) abundant
		layer of bivalve fragments
EOC 9 cm		